CHAPTER 1

INTRODUCTION

Turning is a very important machining process in which a single point cutting tool is used to remove unwanted material from the surface of a rotating cylindrical work piece. The cutting tool is fed linearly in a direction parallel to the axis of rotation. Turning is carried out on lathe that provides the power to turn the work-piece at a given rotational speed and feed to the cutting tool at specified rate and depth of cut. Therefore, three cutting parameters namely cutting speed, feed rate and depth of cut need to be optimized in a turning operation. Turning operation is one of the most important operations used for machine elements construction in manufacturing industries i.e. aerospace, automotive and shipping [1].

Turning is the machining operation that produces cylindrical parts. In its basic form, it can be defined as the machining of an external surface:

- With the work piece rotating.
- With a single-point cutting tool, and
- With the cutting tool feeding parallel to the axis of the work piece and at a distance that will remove the outer surface of the work.

Whenever two machined surfaces have relative motion with each other, the quality of the surfaces play an important role in the performance and wear of the mating parts. The height, shape, arrangement and direction of these surface irregularities on the work piece depend upon a number of factors such as cutting speed, feed and depth of cut [14]. Turning is the removal of unwanted metal from the outer diameter of a rotating cylindrical work-piece. It is used to reduce the diameter of the work- piece, usually to a specified dimension, and finish the cylindrical work-piece surface. Turning is the machining operation that produces cylindrical parts. In its basic form, it can be defined as the machining of an external work-piece surface.

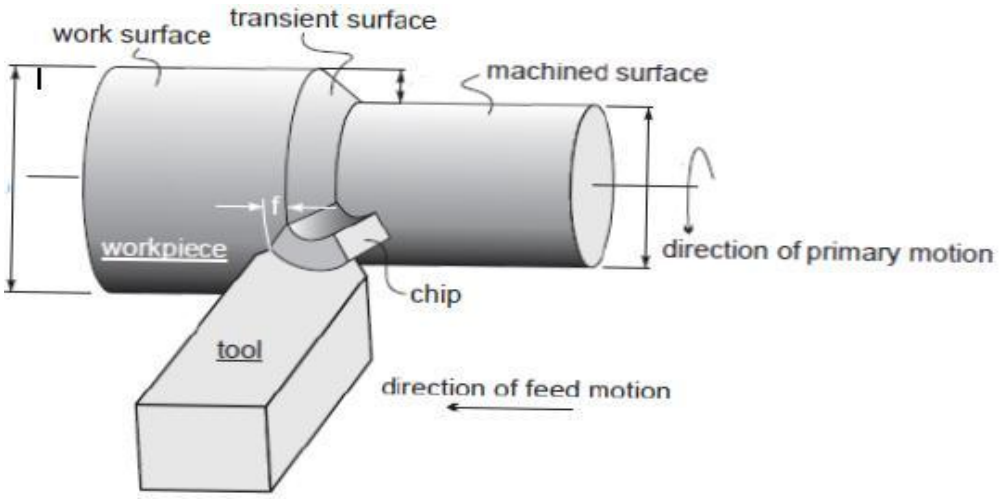

Fig. 1.1: Adjustable parameters in turning operation [12]

Turning is carried out on a lathe machine that provides the power to turn the work-piece at a given rotational speed and feed is given to the cutting tool at specified rate and depth of cut. Therefore, three cutting parameters namely cutting speed, feed and depth of cut need to be determined in the turning operation [14]. The purpose of turning operation is to remove unwanted material from the work-piece surface and produces better quality of surface finish of the parts. Surface roughness is another important factor to evaluate machining performance. Proper selection of cutting parameters can produce precise and lower surface roughness. So it is needed to optimize the process parameters such as cutting speed, feed and depth of cut to improve the response like material removal rate and surface roughness in a turning operation.

1.1 Turning parameters

The turning parameters such as cutting speed, feed and depth of cut play an important role in the production of quality product. Whenever two machined surfaces come in contact with each other, the quality of the mating parts plays an important role in the performance and wear of the mating parts. The height, shape, arrangement and direction of these surface irregularities on the work-piece depend upon number of factors which are given below.

1.1.1 Depth of cut:

It is the thickness of the layer to be removed (in a single pass) from the work-piece or the distance from the uncut surface of the work-piece to the cut surface, expressed in mm. It is important to note, though, that the diameter of the work-piece is reduced by two times the depth of cut because this layer is being removed from both sides of the work-piece.

$$d_{cut} = \frac{D - d}{2} \text{ mm}$$

Here, D and d represent initial and final diameter (in mm) of the job respectively. On the increase of depth of cut, increases the cutting resistance and the amplitude of vibrations as well as increases the temperature at the tool work-piece interface. Therefore, the surface quality of the work-piece deteriorated.

1.1.2 Feed:

Feed is always given to the cutting tool in the turning operation, and it is the rate at which the tool advances along its cutting path. On most power-fed lathes, the feed rate is directly related to the spindle speed and is expressed in mm (of tool advance) per revolution (of the spindle), or mm/rev.

$$F_m = f\, N \text{ mm/min}$$

Here, F_m is the feed in mm per minute, f is the feed in mm/rev and N is the spindle speed in RPM. Experiments show that as the feed rate increases, the surface roughness also increases due to the increase in cutting force and vibration.

1.1.3 Cutting speed:

Speed is always given to the work piece in the turning operation. When it is stated in revolutions per minute (rpm) it tells their rotating speed. But the important feature for a particular turning operation is the surface speed, or the speed at which the work-piece material is moving past the cutting tool. It is simply the product of the rotating speed times the circumference of the work-piece before the cut is started. It is expressed in meter per minute (m/min), and it refers only to the work-piece. Every different diameter on a work-piece will have a different cutting speed, even though the rotating speed remains the same.

$$V = \frac{\pi DN}{1000} \text{ m/min}$$

Here, “V” is the cutting speed in turning operation, “D” is the initial diameter of the work-piece in mm, and N is the spindle speed in rpm. It is found that an increase of cutting speed generally improves the surface quality of the product.

1.2 Surface roughness

The surface roughness was done as coarse, rough, medium and fine. The hand feel and visional inspection were used for theses classifications. There are many ways to define surface roughness depending on its applications like Ra, Rt, Rq, R_k, but roughness average Ra is widely used in industry for the mechanical components for indication of surface roughness, also known as arithmetic aver-age (AA) or centre line average (CLA) [ISO-4287, 1997]. Is the area between surface profile and centre line [13], hence in this study Ra is used for indication of surface roughness.

$$Ra = \frac{1}{L} \int_0^L | Y(x) | dx$$

Whereas L is the sample length, Y(x) is the profile along the direction x. Also

$$Ra = \frac{1}{n} \sum_{i=1}^{n} | y_i |$$

Where n is the total number of samples and Y_i is the height of profile at ith position. Surface roughness plays an important role in product quality. X. Wang [4] focuses on developing an empirical model for the prediction of surface. The model considers the following working parameters: work piece hardness (material), feed, depth of cut, spindle speed [5].

1.3 Material Removal Rate

The material removal rate (MRR) in turning operations is the volume of material or metal that is removed per unit time in mm3/sec. For each revolution of the work piece, a ring shaped layer of material is removed. Material removal rate has been calculated as per following equation.

$$MRR = \pi \times \frac{(D_1^2 - D_2^2)}{4} \times f \times N$$

Here, D1 is the initial and D2 is the final diameter of work-piece, f is the feed rate and N is the spindle speed [3].

$$MRR\ (gm/min) = \frac{W_i - W_f}{t}$$

Where, W_i = Initial weight of work piece material (gm.), W_f = Final weight of work piece material (gm.), t = Time period of trials in minutes [10].

1.4 Selection of work-piece Material

Turning is characterized by gradual material removal in the form of chips. It is provide dimension accuracy and surface quality to the work-piece. Its objective is to fulfill the function requirement of the object, work better, perform better and render longer service life. The chips forming during the turning is an important index of machining [22]. The chips configuration and color is a qualitative measure to check whether ongoing machining is favorable or not favorable. By the chip one can understand the type of material is machining. So if the type of chips are discontinuous it means that the work material behaving brittle. If the chips form are continuous the work material behaving brittle. If the chips are ribbon type continuous it means the work material behaving hard material [12].

EN-31 tool steel material is a hard material. This material is used for ball and roller bearings, spinning tools, bearing rolls, punches and dies. As per its nature, this type of tool steel has high resisting properties against wear and can be used for components which are subjected to sever abrasion, wear or high surface loading, due to its characteristics it is also used in bearing materials. It is also called as bearing material.

CHAPTER 2
LITERATURE REVIEW

The conventional solution to finishing hard material parts (50-70 HRC) has been grinding, but there are a number of befits to the machining of hard materials with a cutting tool. Turning of hard material was early recognized and pioneered by the automotive industry as a means of improving the manufacturing of transmission components. Gear wheel and bearing surface are a great example of early applications converted from grinding to machining [11]. A common method to manufacture parts to a specific dimension involves the removal of excess material by machining operation with the help of cutting tool. Turning process is the one of the methods to remove material from cylindrical and non-cylindrical parts. There are three turning parameters like cutting speed, feed and depth of cut. For better quality of product, the surface roughness, Material removal rate and maximum temperature should be kept in mind. Here presents some papers for this project.

A.Pal et al. (2014) experimental investigated to assess the machinability of hard AISI 4340 steel through mathematical modeling during hard turning (> 45 HRC) and soft turning (< 45 HRC) with TiC mixed alumina ceramic tool. Effect of work-piece hardness and turning parameters (cutting speed, feed and depth of cut) on different responses (chip-tool interface temperature, cutting forces and surface roughness) were analyzed by performing ANOVA technique. They have measured the chip-tool interface temperature with tool-work thermocouple. They have planned the experiment design by central rotatable composite design technique (CCD). They have measured the cutting forces piezoelectric dynamometer. They have used conventional lathe machine. They have observed that the surface roughness decreases with increase in hardness level of work-piece. The reason is the grain size of the work-piece decreases resulting in smaller size of craters on the turned surface due to removal of grains and hence, decreases in roughness value. They have concluded that interface temperature increases with increase in hardness.

S. Harish et al. (2009) studied the potential of cryogenic treatment on toughness of the EN-31 tool steel, the impact behavior of EN-31 tool steel by fractography analysis and to quantify the improvement in hardness. They have used vicker hardness tester to measurement hardness and charpy instrumented impact test with strain gauges to check the impact load. They have concluded that the toughness of different work-pieces of EN-31 tool steel (bearing

steel) after remains the same in charpy impact test. They have also concluded that the microstructure analysis reveals the formation of fine carbide particles in the martensite matrix as a result of tempering. So, cryogenic treatment should be followed by tempering for hardness augmentation and wear resistance improvement.

A. Yadav et al. (2012) focused on the investigation of affect of cutting speed, feed, depth of cut on hardness of work-piece in turning. They selected EN-8 as experimental work-piece material. They adopt Taguchi's method in the design of experiments for designing process and applying maximize S/N ratio for analyzing the experiments data. For measuring of hardness, they use Rockwell hardness tester. In their analysis they observed that as the cutting speed increases, hardness decreases, but after further increasing the cutting speed, the hardness also increases. They have observed that the hardness of work-piece increases as the feed rate changed from 0.15 mm/rev to 0.3 mm/rev and 0.3 mm/rev to 0.45 mm/rev, again they observed that as the depth of cut increases from 0.8 mm to 1.00 mm but as it further increases hardness decreases. They have performed the machining operation on medium duty conventional lathe machine.

A.Belloufi et al. (2013) presented a new optimization technique (hybrid genetic algorithm with the help of sequential quadratic programming) to determine the optimal turning parameters that minimize the production unit cost in multi pass turning processes. They have not selected any specific work-piece and tool. They have checked the result of their proposed technique by comparing it with literature results. They have proposed their technique to implement any kind of work-piece material and any kind of tool.

P. P. Kulkarni et al. (2014) determined the effect of cutting fluids and turning parameters on chip formation mode and cycle time in turning of EN-24 alloy steel and EN-31tool steel. They have employed soluble oil and vegetable oil (palm oil) as cutting fluids. They have found that that the surface finish and material removal rate improved by using vegetable oil. Vegetable oil is much better compare to soluble oil in terms of color and shape of chips. They have observed that at higher speed, the ribbon type continuous chips produced under wet and dry condition and at lower speed and feed, less tubular and continuous helical shaped chips developed. They have concluded that ribbon type continuous chips at higher cutting speed of 710rpm with burnish blue color. They have performed the experiments on

conventional lathe machine and they have selected very small values of level of independent variables.

L. B. Abhang et al. (2010) focused on the optimization of the power consumption during turning operation. They used EN-31 tool steel material as the work-piece for their experiments. They used ANOVA for analysis of experimental data. They find feed rate has the most significant effect on the power, followed by depth of cut, tool nose radius and cutting speed. They also concluded that at the minimum value of cutting speed, feed rate, depth of cut and tool nose radius, the power consumption has the lowest value and vice-versa. They have used conventional lathe machine. They have not got the optimum values of turning parameters.

S. Thamizhmanii et al. (2007) investigated the optimum turning parameters for minimum surface roughness in turning SCM 440 alloy steel by using Taguchi method and ANOVA. They have used coated ceramic cutting tool. They have found that depth of cut is a dominating factor to produce lower surface roughness followed by feed. They also observed that the cutting speed has not play a major role on surface roughness. They have concluded that for minimum surface roughness, the value of depth of cut should be in the range of 1 to 1.5mm. They used soft material in comparison of EN-31 tool steel. They have selected small value of feed levels.

Panda et al. (2014) studied on hard turning of EN-31 tool steel (55HRC) using TiN/TiCN/Al2O3 multilayer coated carbide inserts through Taguchi design and investigates surface roughness under dry environment. The machining operations were performed on CNC lathe machine. They used coated carbide inserts (TiN / TiCN / Al2O3) for machining. The surface roughness was measured by Taylor Hobson (Surtronic 25) surface roughness tester. They used Taguchi method for designing and optimization. ANOVA used for analysis purpose. They have concluded that the surface quality of machined work-piece can achieve better by using coated carbide inserts. And feed is the most dominant factor in subject to the surface roughness. They have got the optimum value for minimum surface roughness of turning parameters are cutting speed 110 m/min, feed 0.04 mm/rev and depth of cut 0.4 mm. They have selected small value of level of depth of cut and feed.

K. Adarsh Kumar et al. (2012) focused on the analysis of optimum cutting conditions (like cutting Speed, Feed rate, Depth of cut) to get lowest surface roughness of EN-8 in facing operation by regression analysis. They have taken coated ceramic tool for machining the work-piece. They have used multiple regression modeling method for optimization. They measured the surface roughness by using Mitutoyo SJ-310 instrument. Mini-Tab software was used for Regression analysis. They observed that the effect of feed rate is having greater effect as compared to cutting speed, and also observed that as the feed rate increasing, the surface roughness is also increases. They have used conventional lathe machine for machining operations. They have selected only three levels.

H. K. Dave et al. (2012) presents the analysis and optimization of cutting parameters like cutting speed, feed and depth of cut, to get the lowest surface roughness and maximum material removal rate in CNC dry turning by using TiN coated cutting tools. They have taken different grades of EN materials. They have employed Taguchi method for experimental design and ANOVA & s/n ratio approach for analysis purpose. They have observed in their experiments and analysis that for high material removal rate, the depth of cut is a dominating factor and for lower surface roughness, the insert has play a significant role. They also concluded that by increasing the speed, material removal rate will increase and for getting the higher material removal rate, the positive insert is preferred than negative insert. They have selected only two levels of independent variables.

C. R. Barik et al. (2012) focused on the optimization of turning parameters (i.e. cutting speed, feed, depth of cut) by applying the genetic algorithm in CNC turning of EN-31 tool steel, and also analyzed the effect of turning parameters on surface roughness with the help of Response Surface Methodology. They have found in their experiments, as the spindle speed and depth of cut increases, the surface roughness decreases and with increasing the feed rate the surface roughness increases. They have got the optimum value of cutting speed 2000 rpm, feed 0.1 mm/rev and depth of cut 0.1mm. They have selected only three levels of independent variables. The values of depth of cut are very small.

L. B. Abhang et al. (2011) studied on the behavior of turning parameters (like cutting speed, feed and depth of cut) with tool-nose radius and concentration of solid-liquid lubricant, on the surface roughness of EN-31 tool steel during turning operation. They have employed response surface methodology along with design of experiments for design of

process and analysis of variance (ANOVA) for analyze the process parameters. They have found that as the feed and depth of cut increases, the surface roughness increases but while cutting speed, tool-nose radius and concentration of solid-liquid lubricant increasing, the surface roughness decreases. They have taken conventional lathe machine for experiments and three levels of independent variables.

A. H. Suhail et al. (2010) experimental studied to analyze the turning parameters on surface roughness and work-piece surface temperature, and then found the optimum value of turning parameters. They have measured the work-piece surface temperature by an infrared thermometer. They employed medium carbon steel AISI 1020 as work-piece material. They have concluded that at1400 rpm cutting speed, 0.05 mm/rev feed and 1.5mm depth of cut give higher surface temperature. They have found that the higher surface temperature gives better surface roughness.

L.B.Abhang et al. (2010) experimentally measured the chip-tool interface temperature during turning of EN-31 tool steel with tungsten carbide inserts. They have measured the chip-tool interface temperature with the help of thermocouple technique. They have used response surface methodology with design of experiments and for analysis of experimental data, they have employed ANOVA. They have concluded that cutting speed is the dominating factor on chip-tool interface temperature. They also concluded that by increasing the cutting speed, feed and depth of cut, the chip-tool interface temperature increases but if tool-nose radius increases, the chip-tool interface temperature decreases. They have performed the experiments on conventional lathe machine and they have selected very small values of level of depth of cut. They have taken only three levels of independent variables.

S. R. Das et al. (2012) presented minimum tool wear and low work-piece surface temperature by optimizing the turning parameters in dry turning of AISI D2 steel. They have used Taguchi and ANOVA for optimization. AISI steel is widely uses in manufacturing tool in mould industries. They have used CNC machine. They have measured the wok-piece surface temperature with the help of infrared thermometer. They have selected three levels of independent variables. They have found that at 150 m/min cutting speed, 0.5 mm depth of cut and 0.25 mm/rev feed, the tool wear and work-piece surface temperature are lower. They

have concluded that depth of cut and cutting speed is the major factor in case of tool wear and the lower surface temperature gives minimum tool wear on the cutting tools.

S. S. Acharya et al. (2014) studied on optimization of surface roughness, material removal rate, machining time in wet and minimum quantity lubricant (MQL) system in turning of hard EN-31 tool steel. They have taken four independent variables like cutting speed, feed, depth of cut and insert nose radius. They have employed response surface methodology in design of experiments. They have found that minimum quantity lubrication system reduced the cutting zone temperature properly and very fast. They have concluded that feed rate has played a significant role on surface roughness and depth of cut is a dominating factor in tool wear.

N. Uppal et al. (2013) presented an experimental study on the optimization process of turning parameters for maximize the material removal rate of hardened AISI 4041 die alloy steel during turning operation. They have employed Taguchi's design of experiments and ANOVA in their experiments. They have got the optimum machining condition for MRR with cutting speed (300 rpm), feed rate (0.06 mm/rev), and depth of cut (0.2 mm). They have found that the material removal rate increases by increasing the cutting speed and feed but the material removal rate decreases by increasing the depth of cut. They performed the machining operations on conventional lathe machine.

2.1 Research Gap

In the above research papers, the point is clear that the turning parameters like cutting speed, feed and depth of cut should be optimized so that the product surface finish can be obtained better with maximum material removal rate and with better quality of product. In most research papers, they have used conventional lathe machine. In maximum cases only three levels of independent variables have taken. So variety of experiments is not possible. They have taken very small ranges of independent variables. The temperature analysis at chip-tool interface temperature has not been considered accurately in the previous research work.

2.2 Research Objectives

The objective of this project is to get the optimized value of turning parameters so as to get the minimum value of surface roughness, maximum value of material removal rate and limiting value of maximum temperature of work-piece.

- Preparation of samples of EN-31for experimentation work.
- Conduct of experiment on CNC lathe machine.
- Statistical analysis of turning parameters for the response such as surface roughness, material removal rate and maximum temperature at tool-work-piece interface.
- Optimum selection of process parameters for the response such as surface roughness, material removal rate and maximum temperature at tool-work-piece interface using response surface methodology.

CHAPTER 3

EXPERIMENTAL WORK

The experiments have been conducted on EN-31 tool steel using CNC lathe machine (LL 20T L3) under dry condition. The size of the Work-piece of EN-31 tool steel material is of 20 mm diameter and 100 mm of length. In this project 20 numbers of work-piece have taken.

The composition and mechanical properties of work-piece material is given below

3.1 Material composition and mechanical properties

The material used for the experiments is grade EN-31 steel, which is popularly named as bearing material. It is used in automotive type applications, like axle, bearings, spindle and molding dies etc. En-31 tool steel is a high quality alloy steel, having good ductility and shock resisting properties combined with resistance to wear. This steel is basically uses in bearing production in industry sector. This is also uses in rolling pipe industry as a roller. The versatile properties of EN-31 tool steel render them suitable for applications in manufacturing industries.

Fig 3.1.1: EN-31 work-piece

The chemical composition and Mechanical properties of the En-31 tool steel are shown in the table.

Table 3.1: Chemical composition of EN-31 tool steel

Chemical composition	Min %	Max %
Carbon	0.90	1.02
Silicon	0.10	0.35
Manganese	0.30	0.75
Chromium	1.00	1.60
Phosphorous	0	0.040
Sulphur	0	0.040

Table 3.2: Mechanical properties of EN-31 tool steel

Element	Objective
Tensile Strength	750 N/mm^2
Yield Stress	450 N/mm^2
Elongation	30 %
Density	7.8 Kg/m^3
Hardness	63 HRC

3.2 Selection of tool

To perform the turning operation on CNC lath machine choose the cutting tool coated (TiN) carbides (Tungsten) inserts CNMG 120408-THM-F (80^0 diamond shaped insert). Double-sided 80° rhombic inserts, positive rake angle that varies along the edge to negative in order to prevent chipping. Special design reduces chattering.

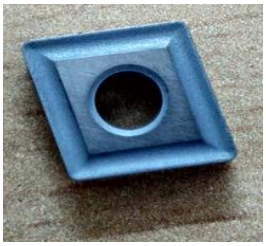

Fig 3.2.1: Coated carbide insert

This insert has the following characteristics:

- Increased speed capability, even when the time in cut is long.
- High metal removal rates, ideal for roughing and semi-roughing operations.
- Fewer machine offsets.
- Longer times between insert indexes.
- Ability to machine harder parts.
- Ability to hold tighter tolerances.

3.3 Experimental setup used

3.3.1 CNC machine

CNC Machining is a process used in the manufacturing sector that involves the use of computers to control machine tools. CNC Machining stands for Computer Numerical Control. A computer program is customized for an object and the machines are programmed with CNC machining language (called G-code, M-codes) that essentially controls all features like feed rate, coordination, location and speeds. With CNC machining, the computer can control exact positioning and velocity. CNC machining is used in manufacturing both metal and plastic parts. There are many advantages to using CNC Machining. The process is more precise than manual machining, and can be repeated in exactly the same manner over and over again. Because of the precision possible with CNC Machining, this process can produce complex shapes that would be almost impossible to achieve with manual machining. CNC Machining is used in the production of many complex three-dimensional shapes. It is because of these qualities that CNC Machining is used in jobs that need a high level of precision or very repetitive tasks.

Figure 3.3.1: CNC Turning Machine

The CNC machine comprises of the computer in which the program is fed for cutting of the metal of the job as per the requirements. Motion is controlled along multiple axes, normally at least two (X and Y), and a tool spindle that moves in the Z (depth). The position of the tool is driven by motors through a series of step down gears in order to provide highly accurate movements, or in modern designs, direct-drive stepper motor or servo motors. Open-loop control works as long as the forces are kept small enough and speeds are not too great. On commercial metalworking machines, closed loop controls are standard and required in order

to provide the accuracy, speed, and repeatability demanded. All the cutting processes that are to be carried out and all the final dimensions are fed into the computer via the program. The computer thus knows what exactly is to be done and carries out all the cutting processes. CNC machine works like the Robot, which has to be fed with the program and it follows all the instructions.

a. Some G-codes used in the experimentation are

G00 - Rapid Positioning

G01 - Linear Interpolation

G02 - Circular Interpolation CW

G03 - Circular Interpolation CCW

G20 - Input in Inches

G21 - Input in Metric

G27 - Reference Point Return Check

G28 - Automatic Zero Return

G29 - Return from Zero Position

b. Some of M-codes used in the experimentation are

M00 - Program Stop

M01 - Optional Program Stop

M02 - Program End

M03 - Spindle Clockwise

M04 - Spindle Counter Clockwise

M08 - Coolant 2 On

M09 - Coolant Off

M30 - End Progarm, Return to Start

c. Programming of CNC machine

Progamme No. 0∅∅∅7

N010 G28 U0.0;

N020 G28 W0.0;

N030 T0707;

N040 G97 S2100 M03;

N050 G00 X50.0 Z50.0;

N060 G00 X20.0 Z10.0;

N070 G01 Z5.0 F0.05;

N080 G01 X19.0;

N090 G01 Z-70.0;

N100 G01 X40.0;

N110 G00 G28 U0.0;

N120 G28 W0.0;

N130 M30

3.3.2 Thermal image Infrared Camera

In this project use a high performance, 320 x 240 infrared camera. Laser Sharp Auto Focus - get consistently in-focus images every single time. This instrument utilizing precision laser technology, focus on the target with pinpoint accuracy and get the correct image and temperature measurements, where needed. This instrument captures visual and infrared images – only with Fusion technology with Auto Blend mode faster communication with wireless image transfer directly to PC.

Fig 3.3.2: Infrared Camera for thermal Image

It is One-handed, easy-to-use interface Touch screen Display (Capacitive) 8.9 cm (3.5 in) diagonal landscape color VGA (640 x 480) LCD with backlight for quick menu navigation Capture additional digital images to show location or additional site details with Annotation System Voice recording and annotation gets additional details saved with the image file. It has optional interchangeable lenses for greater flexibility in additional applications Rechargeable, field replaceable smart batteries with five-segment LED display to show charge levels High-temperature measurement up to 1200°C, 5 MP industrial-performance digital camera for high definition image quality.

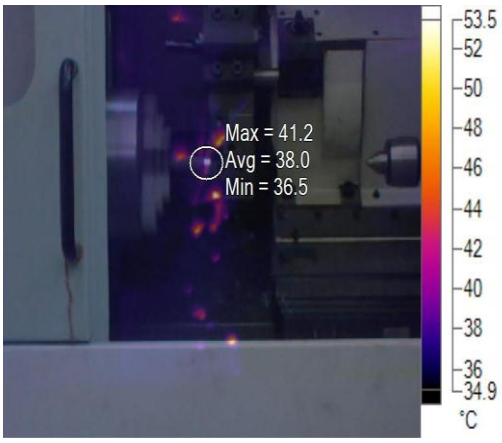

Fig 3.3.3: Infrared camera picture

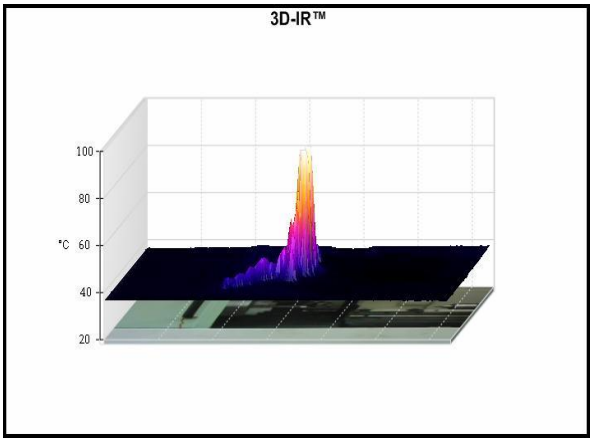

Fig 3.3.4: 3D graph generate by software

Table 3.3.1: Image Info generate by software

Sl. No.	Pareameter	Reading
1	Background Temperature	25.0°C
2	Emissivity	0.95
3	Transmission	1.00
4	Average temperature	36.4°C
5	Image range	35.4°C to 54.8°C
6	Camera Model	Ti400
7	IR sensor size	320 x 240
8	Camera manufacturer	Fluke Thermography

Table 3.3.2: Reading of Image Markers

Sl. No.	Avg. temp	Min. temp.	Max. temp.	Emissivity	Background temp.	St. Dev.
1	38.0°C	36.5°C	41.2°C	0.95	25.0°C	1.05

3.3.3 Surface roughness analyzer

The major output parameter of this project is Surface roughness. For measuring the surface roughness, employed taylor hobson's form talysurf Intra profilometer. This profilometer has the features of a full millimeter of range, a wide selection of interchangeable styli and a patented calibration routine, the Intra system is ideal for almost all high precision applications. The picture of calibration setup is shown in fig 3.3.4.

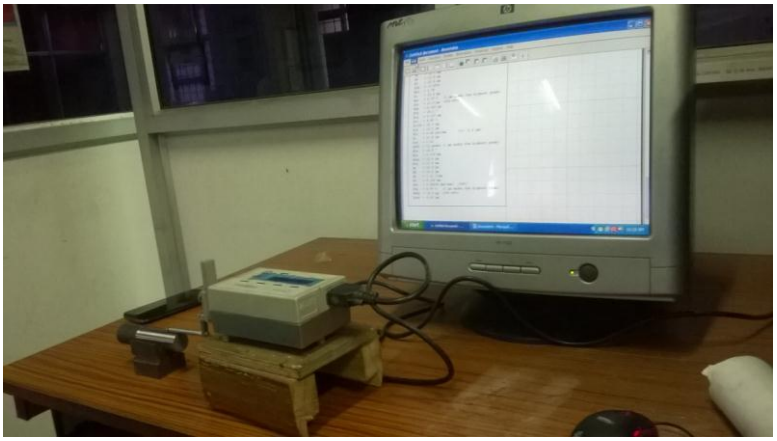

Fig 3.3.5: Setup of Surface roughness measurement

The Talysurf instrument is a portable, self-contained instrument for the measurement of surface texture. The parameter evaluations are microprocessor based. The instrument is powered by non-rechargeable alkaline battery (9V). It is equipped with a diamond stylus having a tip radius 5 μm. The measuring stroke always starts from the extreme outward position. At the end of the measurement the pickup returns to the position ready for the next measurement. The selection of cut-off length determines the traverse length. Roughness measurements, in the transverse direction, on the work pieces have been repeated five times and average of five measurements of surface roughness parameter values has been recorded. The measured profile has been digitized and processed through the dedicated advanced surface finish analysis software Talyprofile for evaluation of the roughness parameters. Surface roughness measurement with the help of stylus has been shown in fig 3.3.6

RPM-2100, Feed- 0.15, Depth OF Cut- 0.25 mm

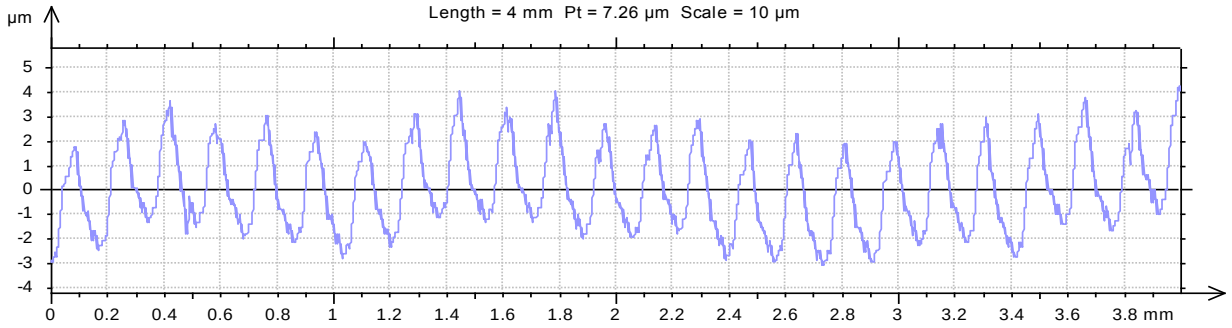

Parameters calculated on the profile DProfile

```
* Parameters calculated on the full length of the
profile.
* A microroughness filtering is used, with a ratio
of 2.5 µm.

Roughness Parameters, Gaussian filter, 0.8 mm

   Ra     = 1.35 µm
   Ra     = 1.35 µm
   Rq     = 1.52 µm
   Rp     = 3.4 µm
   Rv     = 2.52 µm
   Rt     = 5.92 µm
   Rsk    = 0.372
   Rku    = 1.79
   Rz     = 5.92 µm
   Rmr    = 7.08 %    (1 µm under the highest peak)
   Rdc    = 3.17 µm   (20%-80%)
   RSm    = 0.169 mm
   RDq    = 5.82 °
   RLq    = 0.0938 mm
   RLo    = 0.527 %
   RzJIS  = 4.56 µm
   R3z    = 5.66 µm
   RPc    = 5.94 pks/mm        (+/- 0.5 µm)
   Rc     = 4.8 µm
   Rfd    = 1.38
   RHSC   = 19 peaks (1 µm under the highest peak)
   RDa    = 3.95 °
   RLa    = 0.123 mm
   Rmax   = 5.92 µm
   Rtm    = 5.92 µm
   Ry     = 5.92 µm
   RH     = 4.51 µm
   RD     = 5.91 1/mm
   RS     = 0.118 mm
   RVo    = 0.00236 mm3/mm2   (80%)
   RTp    = 7.08 %    (1 µm under the highest peak)
   RHTp   = 3.17 µm   (20%-80%)
   Rrms   = 1.52 µm
```

Fig 3.3.6: Reading of surface roughness by software

CHAPTER 4
STATISTICAL ANALYSIS

4.1 Design of Experiments

Experimental design is a statistical technique that enables an investigator to conduct realistic experiments, analyze data efficiently, and draw meaningful conclusions from the analysis. The aim of scientific research is usually to show the statistical significance of an effect that a particular factor (input parameter/independent variable) exerts on the dependent variable (output/response) of interest. Specifically, the goal of design of experiment is to identify the optimum settings for the different factors that affect the production process. The primary reason for using statistically designed experiments is to obtain maximum information from minimum amount of resources being employed. An experiment (also called run) may be defined as a test in which purposeful changes are made to the input variables of a process so that the possible reasons for the changes in the output/response could be identified. The experimental strategy frequently practiced by the industries is one factor at-a time approach in which the experiments are carried out by varying one input factor and keeping the other input factors constant. This approach fails to analyze the combined effect, when all the input factors vary together which simultaneously govern the experimental response [23]. A well designed experiment is important because the results and conclusions that can be drawn from the experimental response depend to a large extent on the manner in which data were collected.

4.2 Analysis of Variance (ANOVA)

ANOVA is a statistical decision making tool, used to analyze the experimental data, for detecting any differences in the response means of the factors being tested. ANOVA is also needed for estimating the error variance for the factor effects and variance of the prediction error [23]. In general, the purpose of analysis of variance is to determine the relative magnitude of the effect of each factor and to identify the factors significantly affecting the response under consideration (objective function).

4.3 Process variables and their limits

In the present project, spindle speed, feed and depth of cut have been considered as process variables. The process variables with their units (and notations) and their five limits are listed in Table 4.3.1.

Table 4.3.1: Levels of independent variables and their limits

Sl. No.	Independent variables	-1.68	-1.00	0.00	1.00	1.68
1	Cutting speed (rpm)	1500	1800	2100	2400	2700
2	Feed (mm/rev)	0.05	0.10	0.15	0.2	0.25
3	Depth of cut (mm)	0.25	0.50	0.75	1.00	1.25

4.4 CASE STUDY 1 FOR SURFACE ROUGHNESS

After selection of independent variables and their limits, the design of experiments gives the design of process of 20 materials, each having a combination of different levels of factors as shown in table 4.4.1, were carried out.

Table 4.4.1: Design of experiment matrix (coded) for Ra

Sl. No.	Std	Run	Factor 1 A: speed (rpm)	Factor 2 B: Feed (mm/rev)	Factor 3 C: DOC (mm)	Response Ra (μm)
1	20	1	0.00	0.00	0.00	1.29
2	13	2	0.00	0.00	-1.68	1.15
3	7	3	-1.00	1.00	1.00	1.86
4	2	4	1.00	-1.00	-1.00	0.706
5	6	5	1.00	-1.00	1.00	0.92
6	16	6	0.00	0.00	0.00	1.24
7	9	7	-1.68	0.00	0.00	1.44
8	17	8	0.00	0.00	0.00	1.28
9	4	9	1.00	1.00	-1.00	1.16
10	18	10	0.00	0.00	0.00	1.26
11	10	11	1.68	0.00	0.00	0.75
12	14	12	0.00	0.00	1.68	1.7
13	3	13	-1.00	1.00	-1.00	1.55
14	1	14	-1.00	-1.00	-1.00	1.14
15	8	15	1.00	1.00	1.00	1.72
16	19	16	0.00	0.00	0.00	1.31
17	5	17	-1.00	-1.00	1.00	1.32
18	12	18	0.00	1.68	0.00	1.82
19	11	19	0.00	-1.68	0.00	0.9
20	15	20	0.00	0.00	0.00	1.35

In table 4.4.1 the design of matrix in coded form are shown, and their actual value of limits are shown if table 4.4.2

Table 4.4.2: Design of experiment matrix (uncoded) for Ra

Sl. No.	Std	Run	Factor 1 A: speed (rpm)	Factor 2 B: Feed (mm/rev)	Factor 3 C: DOC (mm)	Response Ra (μm)
1	20	1	2100	0.15	0.75	1.29
2	13	2	2100	0.15	0.25	1.15
3	7	3	1800	0.20	1.00	1.86
4	2	4	2400	0.10	0.50	0.706
5	6	5	2400	0.10	1.00	0.92
6	16	6	2100	0.15	0.75	1.24
7	9	7	1500	0.15	0.75	1.44
8	17	8	2100	0.15	0.75	1.28
9	4	9	2400	0.20	0.50	1.16

10	18	10	2100	0.15	0.75	1.26
11	10	11	2700	0.15	0.75	0.75
12	14	12	2100	0.15	1.25	1.7
13	3	13	1800	0.20	0.50	1.55
14	1	14	1800	0.10	0.50	1.14
15	8	15	2400	0.20	1.00	1.72
16	19	16	2100	0.15	0.75	1.31
17	5	17	1800	0.10	1.00	1.32
18	12	18	2100	0.25	0.75	1.82
19	11	19	2100	0.05	0.75	0.9
20	15	20	2100	0.15	0.75	1.35

The experiments were carried out on 20 work-pieces. The experimental data were entered in design of experiment matrix, and then get the design of summary. The design of summary are shown in the table 4.4.3

Table 4.4.3: Design of summary for Ra

Sl. No.	Factor	Name	Units	Type	Subtype	Minimum	Maximum	-1 actual	+1 actual	mean	Std. Dev.
1	A	Speed	rpm	numeric	Continuos	-1.68	1.68	-1.00	1.00	0.00	0.83
2	B	Feed	mm/rev	numeric	Continuos	-1.68	1.68	-1.00	1.00	0.00	0.83
3	C	DOC	mm	numeric	Continuos	-1.68	1.68	-1.00	1.00	0.00	0.83

4.4.1 Result Analysis and Discussion

After design of summary the experimental data are analyzed. During this analysis process get the response range from 0.706 to 1.86, ratio of max to min 2.63456. Then get the summary of quadratic, shown in table 4.4.4. In this summary get the sequential p-value of quadratic less than 0.0001, lack of fit p-value 0.3808, adjusted R-squared 0.9837 and predicted R-squared 0.9531, and this quadratic is suggested. In this evaluation module, a quadratic fit is done. For response surface quadratic model, no aliases (aliases are calculated based on the response selection, taking into account missing data points) found for quadratic model.

Table 4.4.4: Summary of Quadratic for Ra

Sl. No.	Source	Sequential p-value	Lack of fit p-value	Adjusted R-Squared	Predicted R-Squared	
1	Linear	< 0.0001	0.0079	0.8894	0.8320	
2	2FI	0.2495	0.0085	0.8997	0.8554	
3	**Quadratic**	**<0.0001**	**0.3808**	**0.9837**	**0.9531**	**Suggested**
4	Cubic	0.2169	0.8826	0.9883	0.9908	Aliased

Sequential model sum of square (type-I) get in surface roughness analysis process, shown

in table 4.4.5. In this table it is clearly mentioned that the design of experiment suggested for quadratic Vs 2FI model.

Table 4.4.5: Sequential Model Sum of Square (Type-1) for Ra

Sl. No.	Source	Sum Of Squares	df	Mean Square	F Value	p-value prob>F	
1	Mean Vs Total	33.45	1	33.45			
2	Linear Vs Mean	1.85	3	0.62	51.91	< 0.0001	
3	2FI Vs Linear	0.050	3	0.017	1.55	0.2495	
4	**Quadratic Vs 2FI**	**0.12**	**3**	**0.041**	**23.4**	**< 0.0001**	**Suggested**
5	Cubic Vs Quad	9.92×10^{-3}	4	2.48×10^{-3}	1.98	0.2169	Aliased
6	Residual	7.51×10^{-3}	6	1.25×10^{-3}			
7	Total	35.49	20	1.77			

After Sequential model sum of square (type-I) get lack of fit test and model summary statistical in table 4.4.6 and table 4.4.7. In both tables quadratic model is suggested. In lack of fit test the p-value (probability > F) is 0.3808 and F value is 1.33.

Table 4.4.6: Lack of Fit Test for Ra

Sl. No.	Source	Sum Of Squares	df	Mean Square	F Value	p-value prob>F	
1	Linear	0.18	11	0.017	11.08	0.0079	
2	2FI	0.13	8	0.017	11.06	0.0085	
3	**Quadratic**	$\mathbf{9.958\times10^{-3}}$	**5**	$\mathbf{1.992\times10^{-3}}$	**1.33**	**0.3808**	**Suggested**
4	Cubic	3.613×10^{-5}	1	3.613×10^{-5}	0.024	0.8826	Aliased
5	Pure Error	7.483×10^{-3}	5	1.497×10^{-3}			

The desirable value of R-squared is close to one in model summary statistics, table 4.4.7, which is R^2= 99.14% shows that this much percentage of the variability of result is explained by the model. The predicted R-Squared value of 0.9531 is in reasonable agreement with the adjusted R-squared of 0.9837. PRESS stands for predicted residual error sum of squares and it is a measure of how well the model for the experiment is likely to predict the response in new experiments. In this case PRESS is 0.096.

Table 4.4.7: Model Summary Statistics for Ra

Sl. No.	Source	Std. Dev.	R-Squared	Adjusted R-Squared	Predicted R-Squared	PRESS	
1	Linear	0.11	0.9068	0.8894	0.8320	0.34	
2	2FI	0.10	0.9313	0.8997	0.8554	0.29	
3	**Quadratic**	**0.042**	**0.9914**	**0.9837**	**0.9531**	**0.096**	**Suggested**
4	Cubic	0.035	0.9963	0.9883	0.9908	0.019	Aliased

After lack of fit test and model summary statistical, get analysis of variance (ANOVA) for response surface quadratic model, shown in table 4.4.8. In this table get the lack of fit, not

significant and other sources are getting significant. On lack of fit, the F value and p-value (probability > F) are 1.33 and 0.3808 (> 0.05). The lack of fit F-value of 1.33 implies the lack of fit is not significant relative to the pure error. Non significant lack of fit is good. This is desirable as it indicates that the terms in the model have significant effect on the response. This implies that the model could fit and it is adequate. Cutting speed, feed, depth of cut and other sources have p-value less than 0.05. After examination of F-values in this table indicate that the variables, cutting speed (A), feed (B) and depth of cut (C), AB, AC, BC, A^2, B^2, C^2 are significant at 95% confidence level. To ensure the validity of lack of fit test, the degree of freedom for lack of fit should be minimum 3 (< 5) and for pure error minimum 4 (< 5).

Table 4.4.8: Analysis of Variance (ANOVA) for Ra

Sl. No.	Source	Sum of Squares	df	Mean Square	F Value	p-value prob.>F	
1	Model	2.02	9	0.22	128.71	< 0.0001	Significant
2	A-Speed	0.47	1	0.47	267.55	< 0.0001	Significant
3	B-Feed	1.03	1	1.03	590.78	< 0.0001	Significant
4	C-DOC	0.35	1	0.35	201.17	< 0.0001	Significant
5	AB	0.012	1	0.012	6.62	0.0277	Significant
6	AC	0.010	1	0.010	5.78	0.0370	Significant
7	BC	0.028	1	0.028	16.24	0.0024	Significant
8	A^2	0.066	1	0.066	37.81	0.0001	Significant
9	B^2	9.778×10^{-3}	1	9.778×10^{-3}	5.61	0.0394	Significant
10	C^2	0.035	1	0.035	19.86	0.0012	Significant
11	Residual	0.017	10	1.744×10^{-3}			
12	**Lack of Fit**	**9.958×10^{-3}**	**5**	**1.992×10^{-3}**	**1.33**	**0.3808**	**Not significant**
13	Pure Error	7.483×10^{-3}	5	1.497×10^{-3}			
14	Cor Total	2.04	19				

Final Equation in terms of coded factors:

The experimental results were used to develop the mathematical models using response surface methodology (RSM). The proposed first order regression model developed from the above functional relationship using response surface method is as follows:

$Ra = +1.29 – 0.18 *A + 0.27 *B + 0.16 *C + 0.038 *A *B + 0.036 *A *C + 0.060 *B *C – 0.068 *A^2 + 0.026 *B^2 + 0.049 *C^2$

Surface Roughness, Ra = + (1.29) – (0.18 * Cutting Speed) + (0.27 * feed) + (0.16 * Depth of Cut) + (0.038 * Cutting Speed * Feed) + (0.036 * Cutting Speed * Depth of Cut) + (0.060 * Feed *Depth of Cut) – (0.068 *Cutting $Speed^2$) + (0.026 * $Feed^2$) + (0.049 *Depth of Cut^2)

While compare the predicted value with the actual (observed) value, there is a discrepancy. This is called residual. For statistical purposes it's assumed that residual are normally distributed and independent with constant variance. For checking the statistical, normal plot of residual is recommended. The residuals, calculated from the difference of actual versus predicted response, can be plotted on Normal probability paper [21]. If the residuals are normally distributed, they will all fall in a line on this special paper. In this case, the deviations from linear are very minor, so it supports the assumption of normality.

The normal probability plot of residuals for surface roughness is illustrated in Fig 4.4.1. It is expected that data from experiments form a normal distribution. It reveals that the residual fall on a straight line, implying that the errors (residuals) are spread in a normal distribution. Here a residual means difference in the observed value (obtained from the experiment) and the predicted value or fitted value [9]. This is also, confirmed by the variations between the experimental results and model predicted values analyzed through residual graphs.

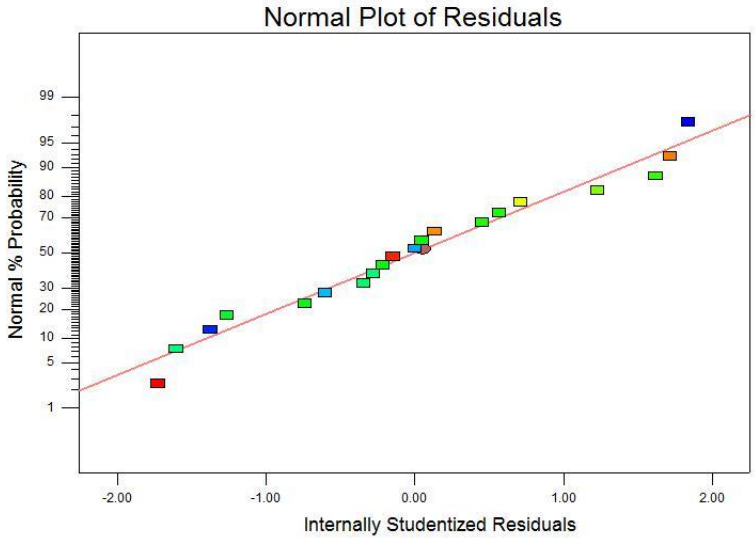

Fig 4.4.1: Normal Plot of Residual for Ra

The actual and predicted plot shows how well the model fits the data. As seen from the fig 4.4.2, all the data lying on the diagonal line. It implies that this model is fit and gives the desired response.

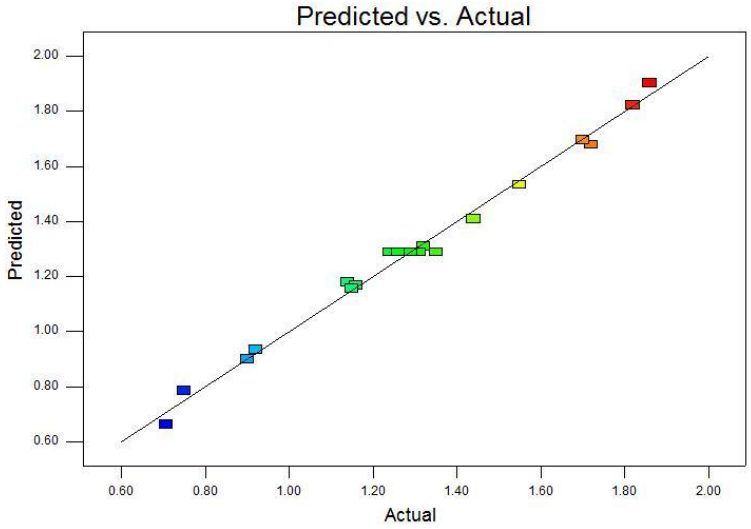

Fig 4.4.2: Predicted Vs Actual for Ra

To show the effect of independent variables like cutting speed, feed and depth of cut plotted individually graph with respect to response surface roughness. These plots are show in fig 4.4.3, fig 4.4.4 and fig 4.4.5.

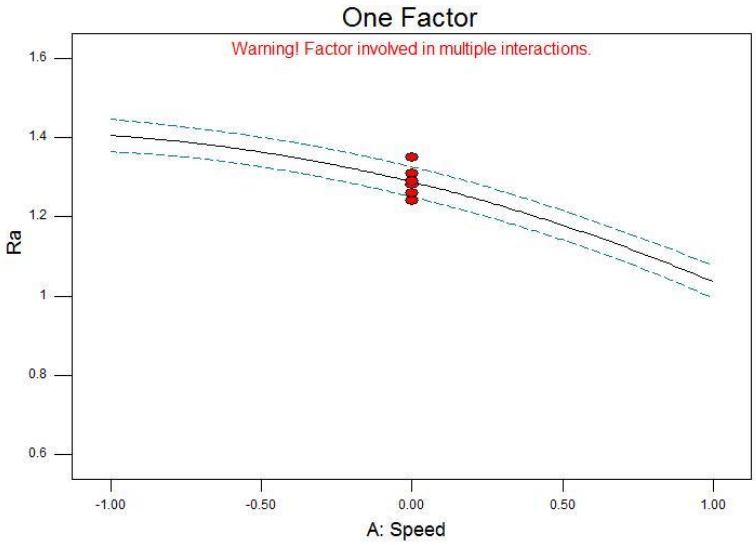

Fig 4.4.3: One Factor-Cutting speed for Ra

In one factor-cutting speed (fig 4.4.3) plot, the behavior of one independent variable cutting speed is showing with response surface roughness. It implies that as the speed increases surface roughness decreases.

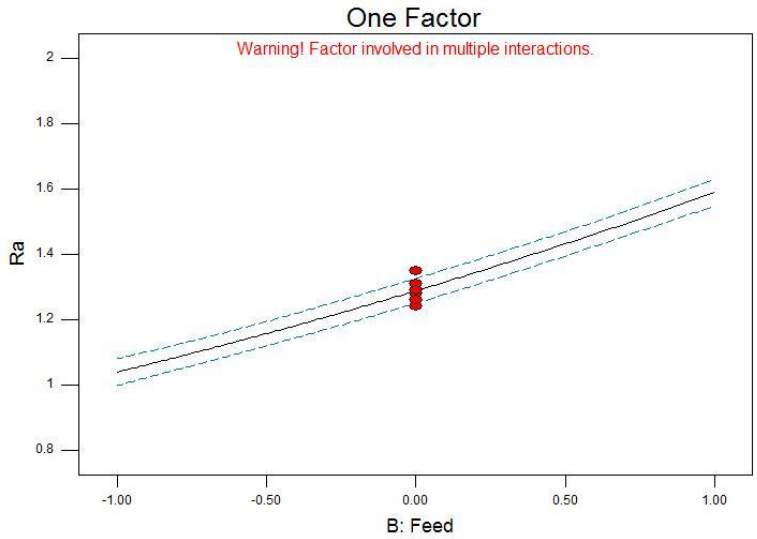

Fig 4.4.4: One Factor-Feed for Ra

The behavior of second independent variable feed is showing with response surface roughness (fig 4.4.4). It implies that as the feed increases surface roughness increases. The behavior of third independent variable depth of cut is showing with response surface roughness (fig 4.4.5). It implies that as the depth of cut increases surface roughness increases.

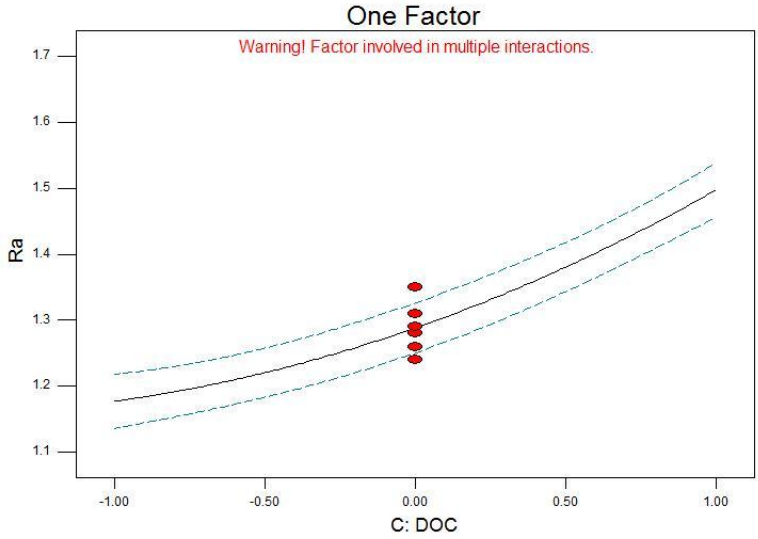

Fig 4.4.5: One Factor-Depth of cut (DOC) for Ra

The graph between cutting speed, feed and depth of cut versus surface roughness have been plotted at one point in perturbation, shown in fig 4.4.6. It implies that as the cutting speed increases, the surface roughness decreases but by increasing the depth of cut and feed, the surface roughness decreases.

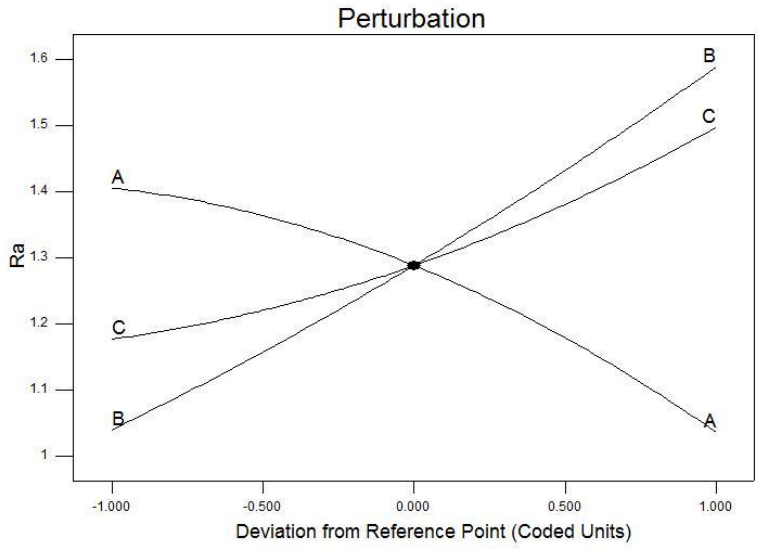

Fig 4.4.6: Perturbation for Ra

Both contour plot and surface 3D plots help to understand the nature of the relationship between the two factors (Cutting speed, feed and depth of cut) and the response (Surface roughness).To convert the experimental data into informative map with quantitative information about the model uses response contour plot. Contour plot is generated for two factors. The typical application of the contour plot is in determining settings that will maximize (or minimize) the response variable. It can also be helpful in determining settings that result in the response variable hitting a pre-determined target value. The contour plots for two different independent variables and response surface roughness are shown in fig 4.4.7, fig 4.4.8 and fig 4.4.9.

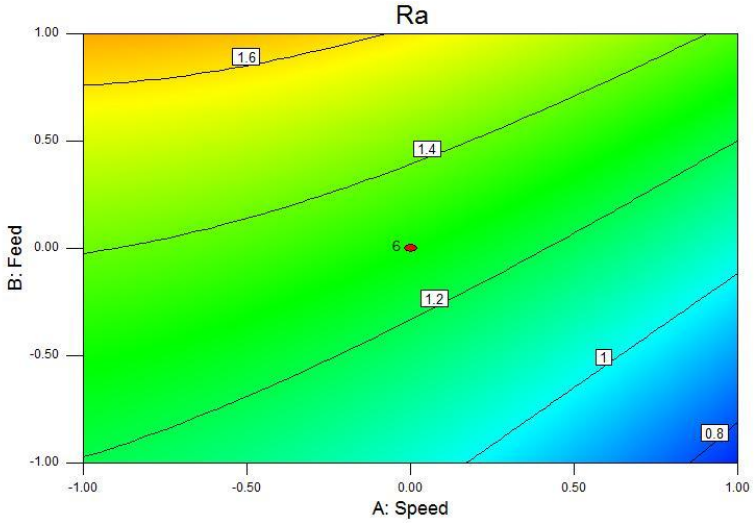

Fig 4.4.7: Response contour plot between Cutting speed and Feed for Ra

The contour plots for two different independent variables (cutting speed and feed) and response surface roughness are shown in fig 4.4.7.

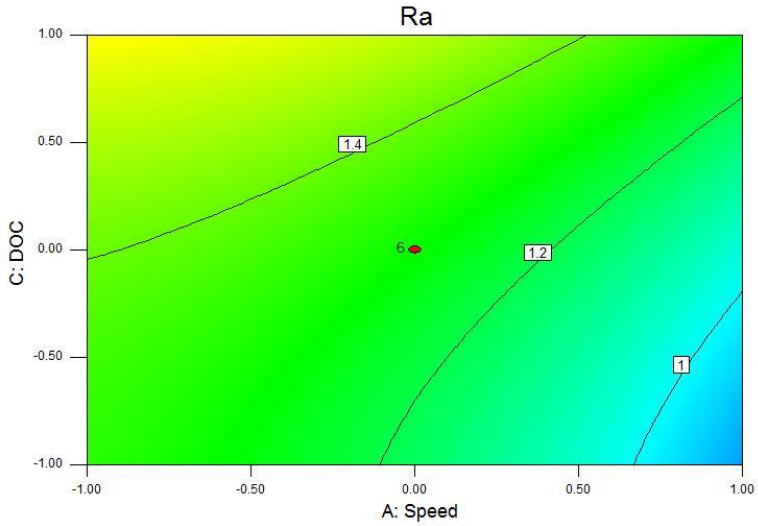

Fig 4.4.8: Response contour plot between Cutting speed and depth of cut for Ra

The contour plots for two different independent variables (cutting speed and depth of cut) and response surface roughness are shown in fig 4.4.8. The contour plots for two different independent variables (Feed and depth of cut) and response surface roughness are shown in fig 4.4.9.

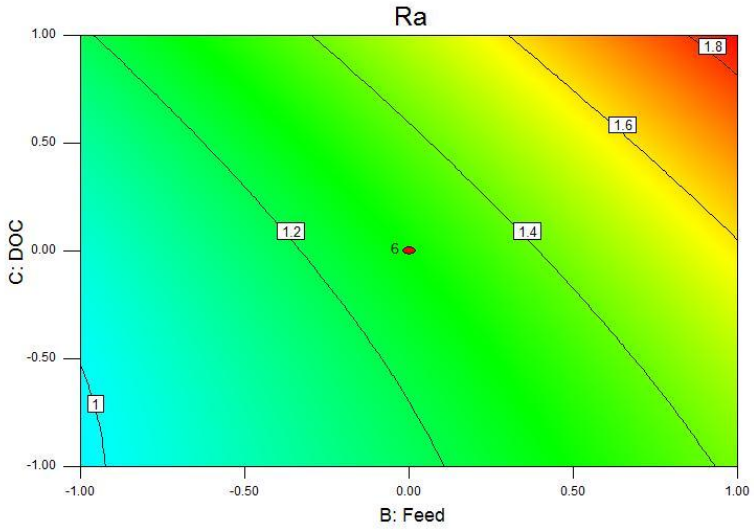

Fig 4.4.9: Response contour plot between Feed and Depth of cut for Ra

A response surface plot generally displays a three dimensional view that may provide a clearer picture of the response. If the regression model (first order model) contains only the main effect and no interaction, the fitted response surface will be a plane (contour lines will be straight). If the model contains interaction effect, the contour lines will be curved and not straight. The contours produced by a second order model will be elliptical in nature. The response surface 3D plot for two different independent variables and response surface roughness are shown in fig 4.4.10, fig 4.4.11 and fig 4.4.12.

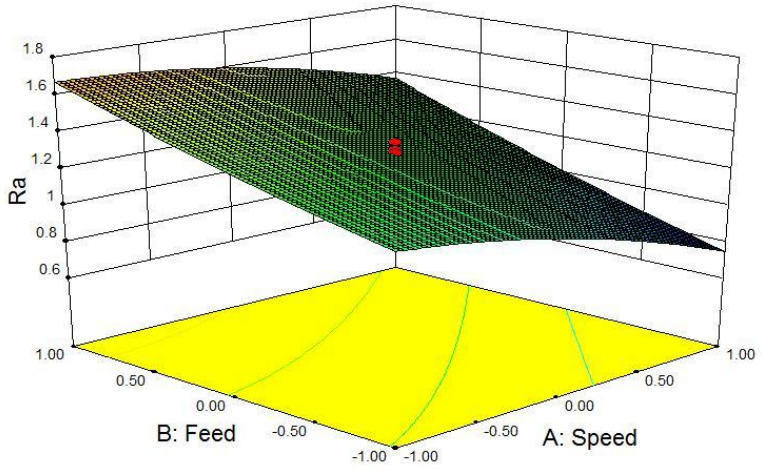

Fig 4.4.10: Response surface 3D plot between Cutting speed and Feed for Ra

In the response surface of 3D graph show the graph between cutting speed and feed (fig 4.4.10), It indicates that the minimum surface roughness is at about 2700 rpm cutting speed and 0.05 mm/rev feed.

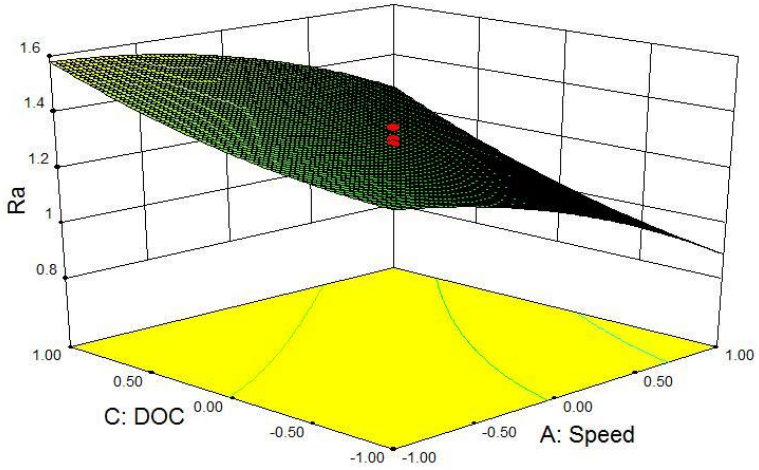

Fig 4.4.11: Response surface 3D plot between Cutting speed and Depth of cut for Ra

In the response surface of 3D graph show the graph between cutting speed and depth of cut (fig 4.4.11), It indicates that the minimum surface roughness is at about 2700 rpm cutting speed and 0.25 mm depth of cut.

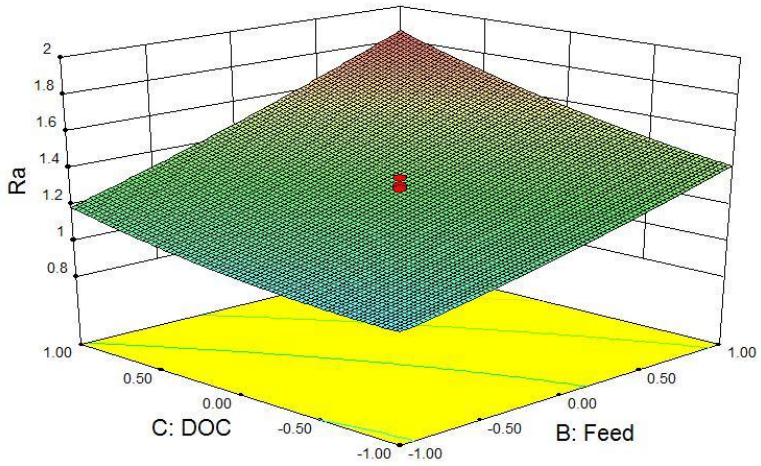

Fig 4.4.12: Response surface 3D plot between Feed and Depth of cut for Ra

In the response surface of 3D graph show the graph between feed and depth of cut (fig 4.4.12), It indicates that the minimum surface roughness is at about 0.05 mm/rev. feed and 0.25 mm depth of cut.

4.4.2 Conclusion

In this case study the effect of turning parameters cutting speed, feed and depth of cut are studied on surface roughness for turning operation on EN-31 tool steel. Analysis of variance is used to study the effect of these parameters and their interaction on surface roughness. In this case study, it is observed that the surface roughness increases with increase in feed followed by depth of cut but decrease with increase in the cutting speed. It is also observed that feed is dominating factor with contribution of 50.49%. The contribution of cutting speed and depth of cut are 23.04% and 17.16% respectively. The minimum value of surface roughness in experiment is 0.706 μm at 2700 rpm cutting speed, 0.05 mm/rev feed and 0.25 mm depth of cut. The maximum value of surface roughness in experiment is 1.86 μm at 2700 rpm cutting speed, 0.05 mm/rev feed and 0.25 mm depth of cut. As per the behavior of contour plots and surface plots get the optimum condition of minimum surface roughness is 2700 rpm cutting speed, 0.05 mm/rev feed and 0.25 mm depth of cut.

4.5 CASE STUDY 2 FOR MRR

4.5.1 MATERIAL REMOVAL RATE

The turning process is carried out on CNC turning machine. The weight of 20 work-pieces has been measured before machining and after machining. The machining time is also noticed during machining. Then material removal rate is calculated by dividing the difference between initial weight and final to the machining time. The experimental result of material removal rate is given in table 4.5.1.

Table 4.5.1: Experiment result for MRR

Sl. No.	Initial weight (gm)	Final weight (gm)	Machine time (sec)	Material removal rate (gm/sec)
1	416.3	400	12	1.357
2	416	411.5	6	0.75
3	419.2	393.7	10	2.55
4	416.5	401.5	15	1.00
5	416	394.7	16	1.33
6	416.2	398	14	1.30
7	418	398	15	1.33
8	417	397.4	13	1.508
9	418	404	9	1.55
10	418.8	401	12	1.48
11	416.6	398	8	2.32
12	417.3	391	10	2.63
13	419	399	17	1.18
14	416	405	22	0.50
15	419	395	8	3.00
16	417	399.6	11	1.581
17	417	393	20	1.2
18	418.4	403.5	7	2.125
19	417	406	34	0.323
20	417.9	400.5	12	1.45

The design of experiments gives the design of process of 20 materials, each having a combination of different levels of factors as shown in table 4.5.2, were carried out.

Table 4.5.2: Design of experiment matrix (coded) for MRR

Sl. No.	Std	Run	Factor 1 A: speed (rpm)	Factor 2 B: Feed (mm/rev)	Factor 3 C: DOC (mm)	Response MRR (gm/sec)
1	20	1	0.00	0.00	0.00	1.357
2	13	2	0.00	0.00	-1.68	0.75
3	7	3	-1.00	1.00	1.00	2.55
4	2	4	1.00	-1.00	-1.00	1.00
5	6	5	1.00	-1.00	1.00	1.33
6	16	6	0.00	0.00	0.00	1.30
7	9	7	-1.68	0.00	0.00	1.33
8	17	8	0.00	0.00	0.00	1.508
9	4	9	1.00	1.00	-1.00	1.55
10	18	10	0.00	0.00	0.00	1.48
11	10	11	1.68	0.00	0.00	2.32
12	14	12	0.00	0.00	1.68	2.63
13	3	13	-1.00	1.00	-1.00	1.18
14	1	14	-1.00	-1.00	-1.00	0.50
15	8	15	1.00	1.00	1.00	3.00
16	19	16	0.00	0.00	0.00	1.581
17	5	17	-1.00	-1.00	1.00	1.2
18	12	18	0.00	1.68	0.00	2.125
19	11	19	0.00	-1.68	0.00	0.323
20	15	20	0.00	0.00	0.00	1.45

In table 4.5.2 the design of matrix in coded form are shown, and their actual value of limits are shown if table 4.5.3

Table 4.5.3: Design of experiment matrix (uncoded) for MRR

Sl. No.	Std	Run	Factor 1 A: speed (rpm)	Factor 2 B: Feed (mm/rev)	Factor 3 C: DOC (mm)	Response MRR (gm/sec)
1	20	1	2100	0.15	0.75	1.357
2	13	2	2100	0.15	0.25	0.75
3	7	3	1800	0.20	1.00	2.55
4	2	4	2400	0.10	0.50	1.00
5	6	5	2400	0.10	1.00	1.33
6	16	6	2100	0.15	0.75	1.30
7	9	7	1500	0.15	0.75	1.33
8	17	8	2100	0.15	0.75	1.508
9	4	9	2400	0.20	0.50	1.55
10	18	10	2100	0.15	0.75	1.48
11	10	11	2700	0.15	0.75	2.32
12	14	12	2100	0.15	1.25	2.63
13	3	13	1800	0.20	0.50	1.18

14	1	14	1800	0.10	0.50	0.50
15	8	15	2400	0.20	1.00	3.00
16	19	16	2100	0.15	0.75	1.581
17	5	17	1800	0.10	1.00	1.2
18	12	18	2100	0.25	0.75	2.125
19	11	19	2100	0.05	0.75	0.323
20	15	20	2100	0.15	0.75	1.45

The experiments were carried out on 20 work-pieces. The experimental data were entered in design of experiment matrix, and then get the design of summary. The design of summary are shown in the table 4.5.4

Table 4.5.4: Design of summary for MRR

Sl. No.	Factor	Name	Units	Type	Subtype	Minimum	Maximum	-1 actual	+1 actual	mean	Std. Dev.
1	A	Speed	rpm	numeric	Continuos	-1.68	1.68	-1.00	1.00	0.00	0.83
2	B	Feed	mm/rev	numeric	Continuos	-1.68	1.68	-1.00	1.00	0.00	0.83
3	C	DOC	mm	numeric	Continuos	-1.68	1.68	-1.00	1.00	0.00	0.83

4.5.2 Result Analysis and Discussion

After design of summary the experimental data are analyzed. During this analysis process get the response range from 0.323 to 3.00, ratio of max to min 9.28793. Then get the summary of quadratic, shown in table 4.5.5. In this summary get the sequential p-value 0.0023, lack of fit p-value 0.2540, adjusted R-squared 0.9689 and predicted R-squared 0.9066, and in this table quadratic is suggested.

Table 4.5.5: Summary of Quadratic for MRR

Sl. No.	Source	Sequential p-value	Lack of fit p-value	Adjusted R-Squared	Predicted R-Squared	
1	Linear	< 0.0001	0.0148	0.8688	0.8033	
2	2FI	0.0701	0.0266	0.9044	0.8525	
3	**Quadratic**	**0.0023**	**0.2540**	**0.9689**	**0.9066**	**Suggested**
4	Cubic	0.1825	0.4162	0.9791	0.7948	Aliased

Sequential model sum of square (type-I) get in material removal rate analysis process, shown in table 4.5.6. In this table it is mentioned that the design of experiment suggested for quadratic Vs 2FI model. Here F-value and p-value are 10.01 and 0.0023 respectively.

Table 4.5.6: Sequential Model Sum of Square (Type-1) for MRR

Sl. No.	Source	Sum Of Squares	df	Mean Square	F Value	p-value prob>F	
1	Mean Vs Total	46.43	1	46.43			
2	Linear Vs Mean	8.20	3	2.73	42.93	< 0.0001	
3	2FI Vs Linear	0.42	3	0.14	2.99	0.0701	
4	**Quadratic Vs 2FI**	**0.45**	**3**	**0.15**	**10.01**	**0.0023**	**Suggested**
5	Cubic Vs Quad	0.090	4	0.023	2.22	0.1825	Aliased
6	Residual	0.061	6	0.010			
7	Total	55.65	20	2.78			

After Sequential model sum of square (type-I) get lack of fit test and model summary statistical in table 4.5.7 and table 4.5.8. In lack of fit test (table 4.5.7) the p-value (probability > F) is 0.2540 and F-value is 1.87.

Table 4.5.7: Lack of Fit Test for MRR

Sl. No.	Source	Sum Of Squares	df	Mean Square	F Value	p-value prob>F	
1	Linear	0.97	11	0.088	8.37	0.0148	
2	2FI	0.55	8	0.069	6.56	0.0266	
3	**Quadratic**	**0.098**	**5**	**0.020**	**1.87**	**0.2540**	**Suggested**
4	Cubic	8.239×10^{-3}	1	8.239×10^{-3}	0.79	0.4162	Aliased
5	Pure Error	0.052	5	0.010			

In model summary statistics, table 4.5.8, the value of R^2= 98.36% shows that this much percentage of the variability of result is explained by the model. The predicted R-Squared value of 0.9066 is in reasonable agreement with the adjusted R-squared of 0.9689. PRESS stands for predicted residual error sum of squares and it is a measure of how well the model for the experiment is likely to predict the response in new experiments. In this case PRESS is 0.86.

Table 4.5.8: Model Summary Statistics for MRR

Sl. No.	Source	Std. Dev.	R-Squared	Adjusted R-Squared	Predicted R-Squared	PRESS	
1	Linear	0.25	0.8895	0.8688	0.8033	1.81	
2	2FI	0.22	0.9346	0.9044	0.8525	1.36	
3	**Quadratic**	**0.12**	**0.9836**	**0.9689**	**0.9066**	**0.86**	**Suggested**
4	Cubic	0.10	0.9934	0.9791	0.7948	1.89	Aliased

After lack of fit test and model summary statistical, get analysis of variance (ANOVA) for response surface quadratic model, shown in table 4.5.9. In this table get the lack of fit and two other terms AB and AC, not significant and other sources are getting significant. On lack of fit, the F value and p-value (probability > F) are 1.87 and 0.2540 (> 0.05). Cutting speed

(A), feed (B), depth of cut (C), BC, A^2, B^2, and C^2 have p-value less than 0.05. In this the term AB (0.5963) and AC (0.4231) have the p-value more than 0.05. Hence these terms are not significant in this table. For fit model these terms should be less than 0.05. So, for fit model go for backward elimination process.

Table 4.5.9: Analysis of Variance (ANOVA) for MRR

Sl. No.	Source	Sum of Squares	df	Mean Square	F Value	p-value prob>F	
1	Model	9.07	9	1.01	66.85	< 0.0001	Significant
2	A-Speed	0.72	1	0.72	47.65	< 0.0001	Significant
3	B-Feed	3.88	1	3.88	257.52	< 0.0001	Significant
4	C-DOC	3.60	1	3.60	238.85	< 0.0001	Significant
5	AB	4.513×10^{-3}	1	4.513×10^{-3}	0.30	0.5963	Not significant
6	AC	0.011	1	0.011	0.70	0.4231	Not significant
7	BC	0.40	1	0.40	26.57	0.0004	Significant
8	A^2	0.23	1	0.23	14.95	0.0031	Significant
9	B^2	0.11	1	0.11	7.61	0.0202	Significant
10	C^2	0.082	1	0.082	5.46	0.0416	Significant
11	Residual	0.15	10	0.015			
12	**Lack of Fit**	**0.098**	**5**	**0.020**	**1.87**	**0.2540**	**Not significant**
13	Pure Error	0.052	5	0.010			
14	Cor Total	9.22	19				

Final Equation in terms of coded factors:

The experimental results were used to develop the mathematical models using response surface methodology (RSM). The proposed first order regression model developed from the above functional relationship using response surface method is as follows:

MRR = +1.45 + 0.23 *A + 0.53 *B + 0.51 *C + 0.024 *A *B – 0.036 *A *C + 0.22 *B *C + 0.13 *A^2 – 0.089 *B^2 + 0.076 *C^2

Material Removal Rate, MRR = +(1.45) + (0.23 * Cutting Speed) + (0.53 * feed) + (0.51 * Depth of Cut) + (0.024 * Cutting Speed * Feed) – (0.036 * Cutting Speed * Depth of Cut) + (0.22 * Feed *Depth of Cut) + (0.13 *Cutting $Speed^2$) – (0.089 * $Feed^2$) + (0.076 *Depth of Cut^2)

The normal probability plot of residuals for material removal rate is illustrated in Fig 4.5.1. It is expected that data from experiments form a normal distribution. This is also, confirmed by the variations between the experimental results and model predicted values analyzed through residual graphs.

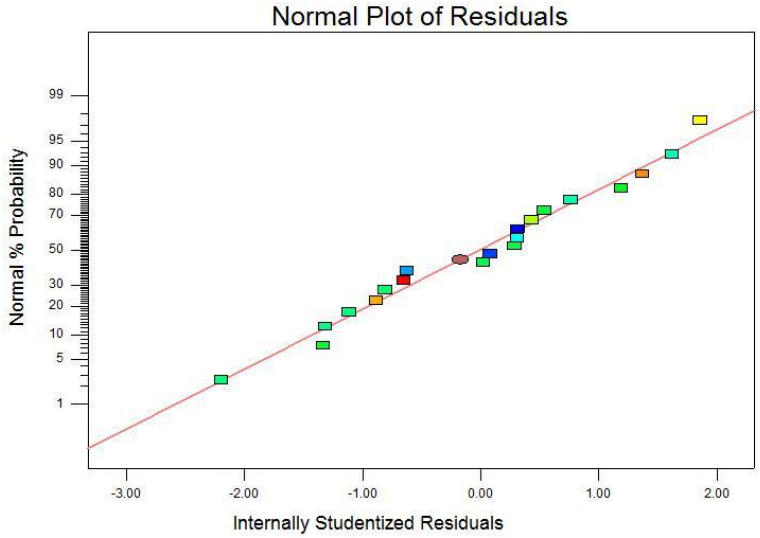

Fig 4.5.1: Normal Plot of Residual for MRR

The actual and predicted plot shows how well the model fits the data. As seen from the fig 4.5.2, all the data lying on the diagonal line.

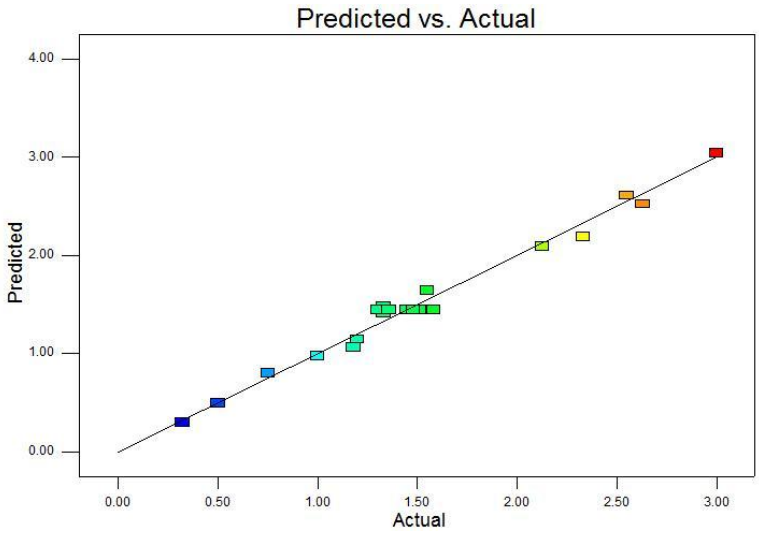

Fig 4.5.2: Predicted Vs Actual for MRR

To show the effect of independent variables like cutting speed, feed and depth of cut plotted individually with respect to response material removal rate. These plots are show in fig 4.5.3, fig 4.5.4 and fig 4.5.5.

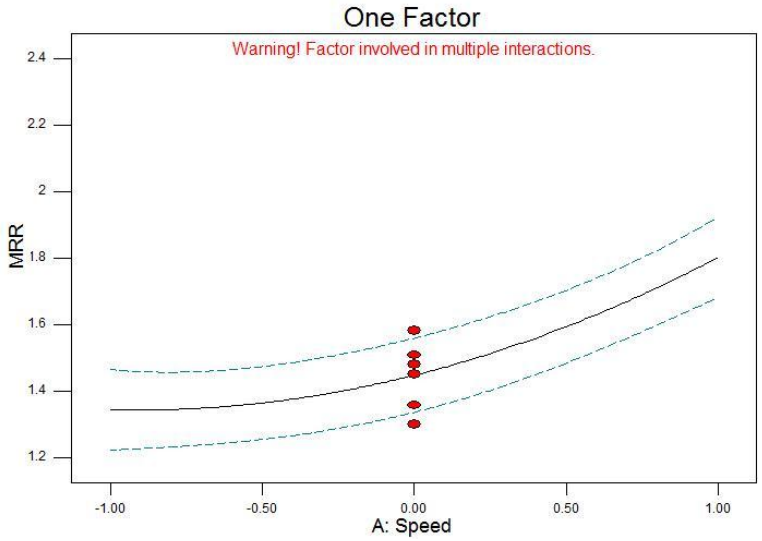

Fig 4.5.3: One Factor-Cutting speed for MRR

In one factor-cutting speed (fig 4.5.3) plot, the behavior of one independent variable cutting speed is showing with material removal rate. It implies that as the speed increases material removal rate is flat but as further cutting speed increases the material removal rate is also increases.

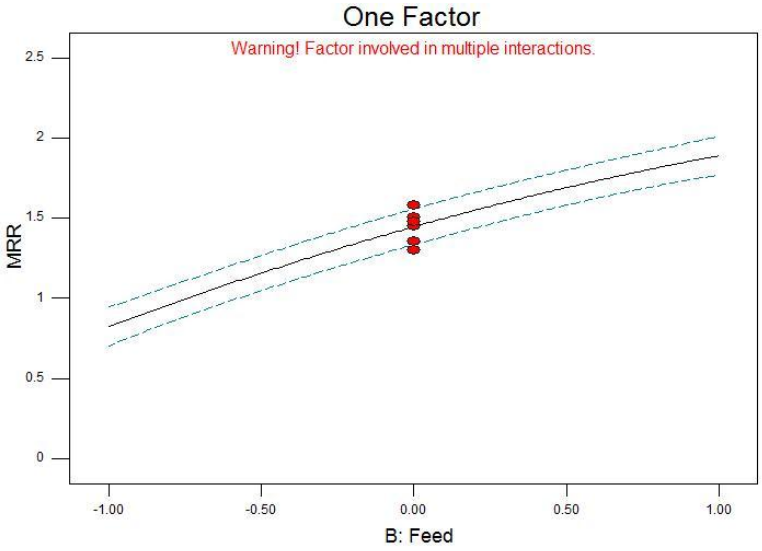

Fig 4.5.4: One Factor-Feed for MRR

The behavior of second independent variable feed is showing with respect to material removal rate (fig 4.5.4). It implies that material removal rate increases by increasing the feed. The behavior of third independent variable depth of cut is showing with respect to material removal rate (fig 4.5.5). It implies that as the depth of cut increases material removal rate increases.

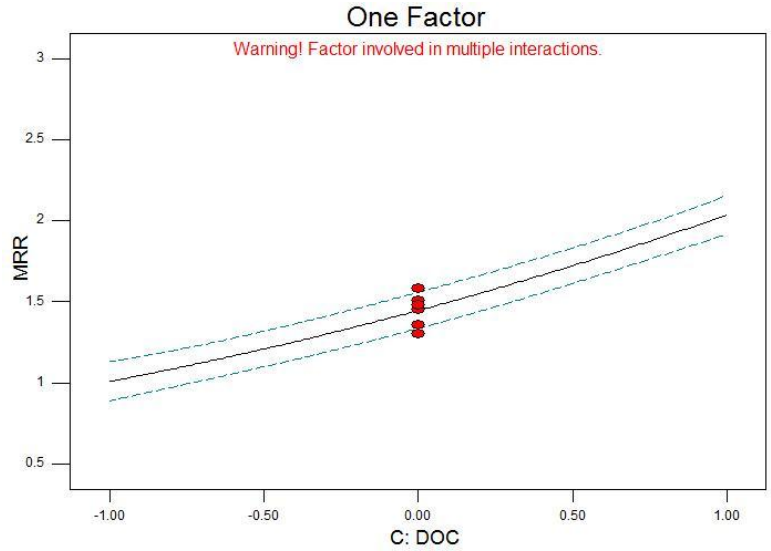

Fig 4.5.5: One Factor-Depth of cut for MRR

The graph between cutting speed, feed and depth of cut versus material removal rate, at a point have been plotted in perturbation, shown in fig 4.5.6. It implies that as the cutting speed increases, the material removal rate is initially flat and then increases but by increasing the depth of cut and feed, the surface roughness increases.

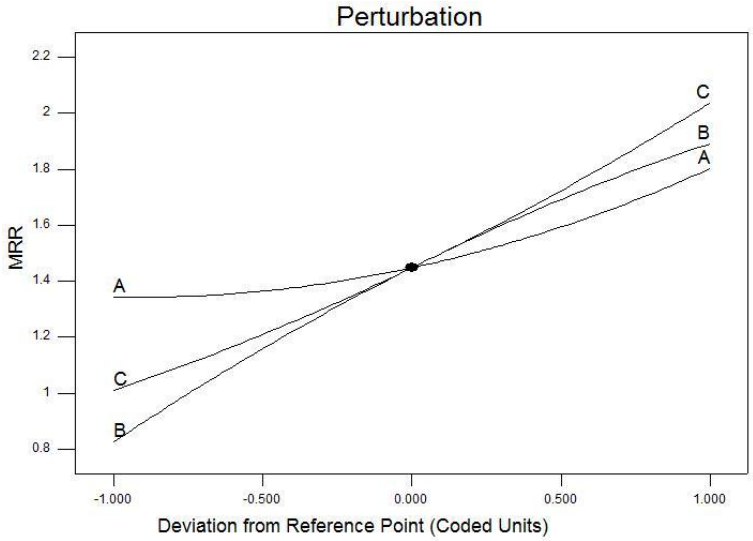

Fig 4.5.6: Perturbation graph for MRR

Both contour plot and surface 3D plots help to understand the nature of the relationship between the two factors (Cutting speed, feed and depth of cut) and the response (material removal rate).To convert the experimental data into informative map with quantitative information about the model uses response contour plot. The contour plots for two different independent variables and response material removal rate are shown in fig 4.5.7, fig 4.5.8 and fig 4.5.9. The response contour plot between cutting speed and feed is shown in fig 4.5.7.

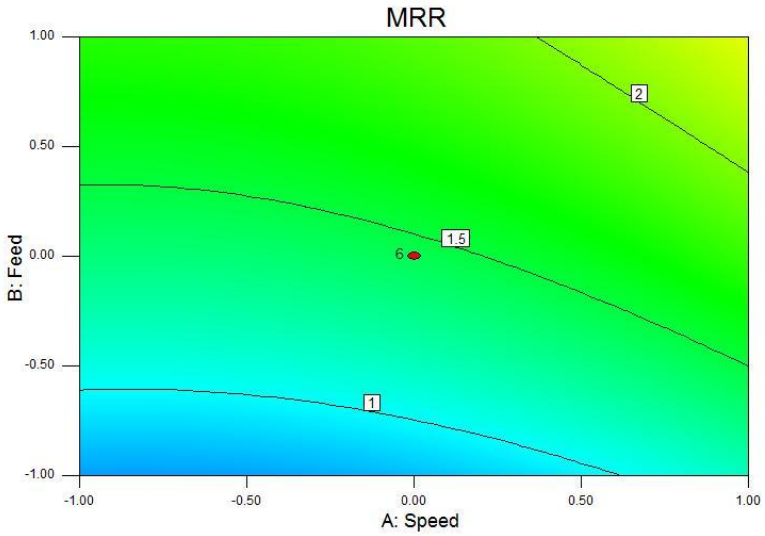

Fig 4.5.7: Response contour plot between Cutting speed and Feed for MRR

The response contour plot between cutting speed and depth of cut for material removal rate is shown in fig 4.5.8.

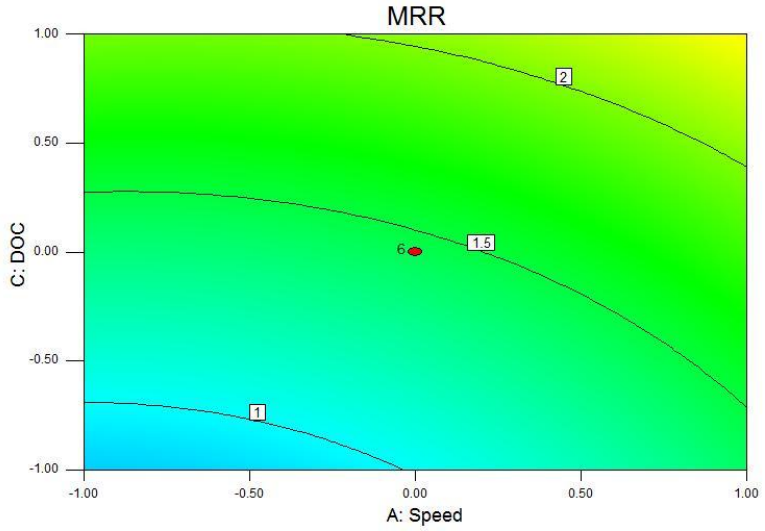

Fig 4.5.8: Response contour plot between Cutting speed and Depth of cut for MRR

The response contour plot between feed and depth of cut for material removal rate is shown in fig 4.5.9.

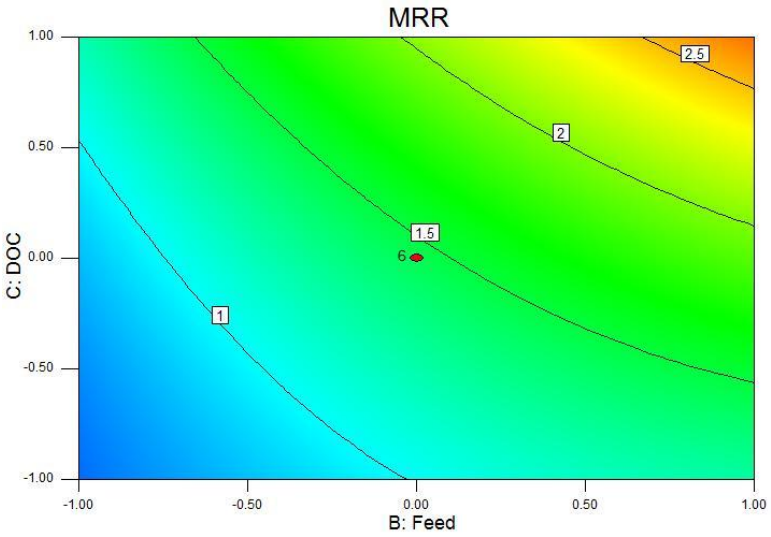

Fig 4.5.9: Response contour plot between Feed and Depth of cut for MRR

The response surface 3D plot for two different independent variables and response material removal rate are shown in fig 4.5.10, fig 4.5.11 and fig 4.5.12.

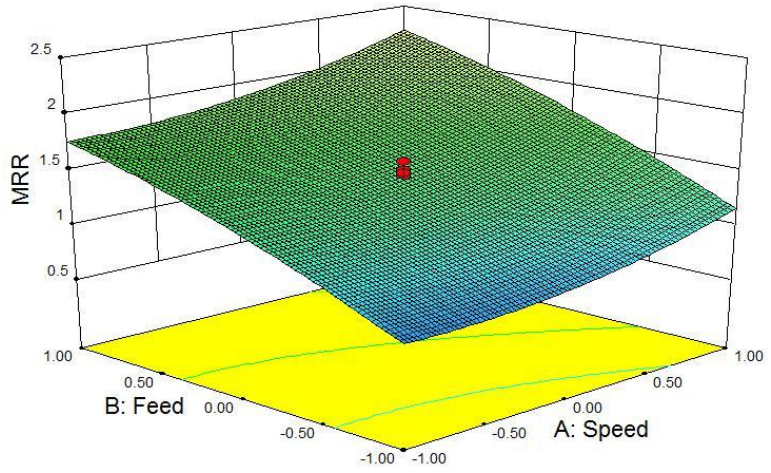

Fig 4.5.10: Response surface 3D plot between Cutting speed and Feed for MRR

The response surface 3D graph between cutting speed and feed for material removal rate is shown in fig 4.5.10.

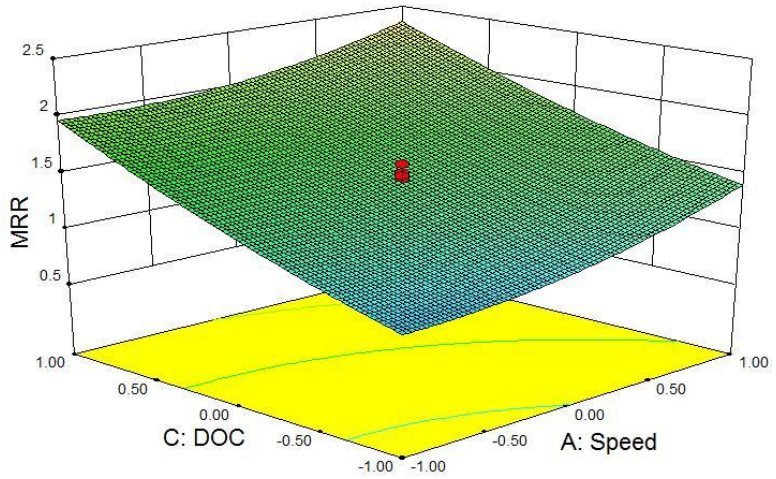

Fig 4.5.11: Response surface 3D plot between Cutting speed and Depth of cut for MRR

The response surface 3D graph between cutting speed and depth of cut for material removal rate is shown in fig 4.5.11.

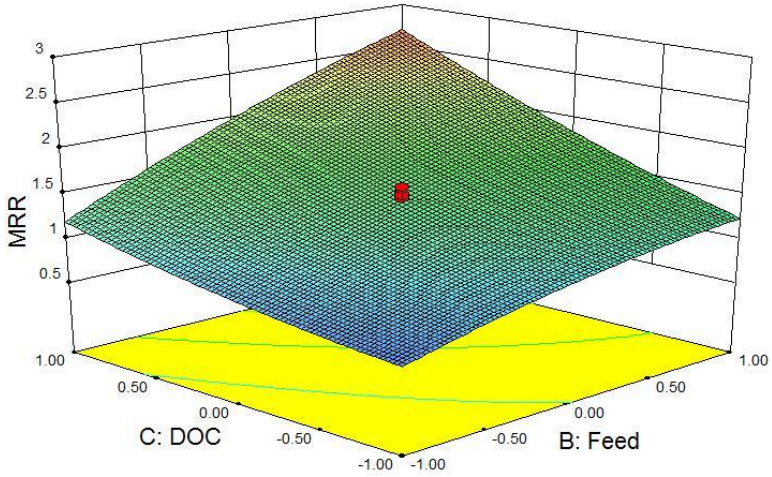

Fig 4.5.12: Response surface 3D plot between Feed and Depth of cut for MRR

The response surface 3D graph between feed and depth of cut for material removal rate is shown in fig 4.5.12.

4.5.3 Backward Elimination Process

The fit summary recommends that the quadratic model is statistically significant for analysis material removal rate. For the appropriate fitting of the model of material removal rate, the non-significant terms AB and AC (p-value is greater than 0.05) are eliminated by the backward elimination process. The term AB and AC have been removed by reduction of model by using Backward Elimination Regression with Alpha to exit = 0.100. During backward elimination process, get forced terms intercept and ANOVA table, which are shown in table 4.5.10 and table 4.5.11.

Table 4.5.10: Forced Terms Intercept for MRR

Sl. No.	Removed	Coefficient Estimate	T for H_0 Coeff = 0	Prob > |t|	R – Squared	MSE
1	AB	0.024	0.55	0.5963	0.9832	0.014
2	AC	-0.036	-0.86	0.4065	0.9820	0.014

Table 4.5.11: Analysis of Variance (ANOVA) after Backward Elimination process

Sl. No.	Source	Sum of Squares	df	Mean Square	F Value	p-value prob>F	
1	Model	9.05	7	1.29	93.63	< 0.0001	
2	A-Speed	0.72	1	0.72	52.00	< 0.0001	
3	B-Feed	3.88	1	3.88	281.01	< 0.0001	
4	C-DOC	3.60	1	3.60	260.64	< 0.0001	
5	BC	0.40	1	0.40	29.00	0.0002	
6	A^2	0.23	1	0.23	16.31	0.0016	
7	B^2	0.11	1	0.11	8.30	0.0138	
8	C^2	0.082	1	0.082	5.96	0.0311	
9	Residual	0.17	12	0.014			
10	**Lack of Fit**	**0.11**	**7**	**0.016**	**1.54**	**0.3275**	**Not significant**
11	Pure Error	0.052	5	0.010			
12	Cor Total	9.22	19				

After backward elimination process, get analysis of variance (ANOVA) for response surface quadratic model, shown in table 4.5.10. In this table get the lack of fit, not significant and other sources are getting significant. The model F-value of 93.63 implies the model is significant. There is only a 0.01% chance that a “model F-value” this large could occur due to noise. On lack of fit, the F value and p-value (probability > F) are 1.54 and 0.3275 (> 0.05). This is desirable as it indicates that the terms in the model have significant effect on the response. This implies that the model could fit and it is adequate. Cutting speed (A), feed (B), depth of cut (C), BC, A^2, B^2, and C^2 have p-value less than 0.05. If there are many insignificant model terms (not counting those required to support hierarchy) model reduction may improve the model. The lack of fit F-value of 1.54 implies the lack of fit is not significant relative to the pure error. There is a 32.75% chance that a “Lack of fit F-value” this large could occur due to noise. Non significant lack of fit is good, as it indicate the model is fit.

Table 4.5.12: Other parameters for MRR

Parametrs	Value	Parametrs	Value
Std. Dev.	0.12	R-Squared	0.9820
Mean	1.52	Adj R-squared	0.9715
C.V.%	7.71	Pred R-Squared	0.9390
PRESS	0.56	Adeq Precisior	37.131

The "Pred R-Squared" of 0.9390 is in reasonable agreement with the "Adj R-Squared" of 0.9715. "Adeq Precision" measure the signal to noise ratio greater than 4 is desirable. This ratio of 37.131 indicates an adequate signal. This model can be used to navigate the design space.

Final Equation in terms of coded factors:

After eliminating the non-significant terms, the final response equation for material removal rate is given as follows

$MRR = +1.45 + 0.23 *A + 0.53 *B + 0.51 *C + 0.22 *B *C + 0.13 *A^2 – 0.089 *B^2 + 0.076 *C^2$

Material Removal Rate, MRR = +(1.45) + (0.23 * Cutting Speed) + (0.53 * feed) + (0.51 * Depth of Cut) + (0.22 * Feed *Depth of Cut) + (0.13 *Cutting Speed^2) – (0.089 * Feed^2) + (0.076 *Depth of Cut^2)

The normal probability plot of residuals for material removal rate after backward elimination process is illustrated in Fig 4.5.13. It is expected that data from experiments form a normal distribution. It reveals that the residual fall on a straight line, implying that the errors (residuals) are spread in a normal distribution. This is also, confirmed by the variations between the experimental results and model predicted values analyzed through residual graphs.

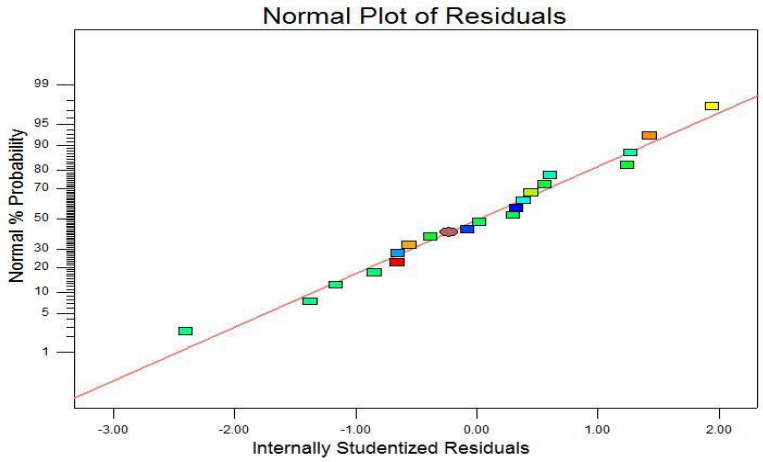

Fig 4.5.13: Normal Plot of Residual for MRR after Backward Elimination

After normal plot of residual get the actual and predicted plot after backward elimination process. The actual and predicted plot shows how well the model fits the data. As seen from the fig 4.5.14, all the data lying on the diagonal line. It implies that this model is fit and gives the desired response.

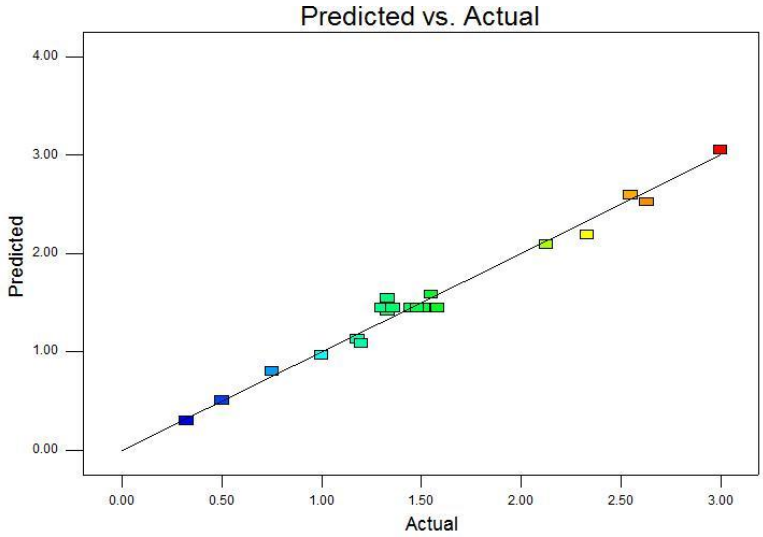

Fig 4.5.14: Predicted Vs Actual for MRR after Backward Elimination

To show the effect of independent variables like cutting speed, feed and depth of cut plotted individually with respect to response material removal rate after backward elimination process. These plots are show in fig 4.5.15, fig 4.5.16 and fig 4.5.17.

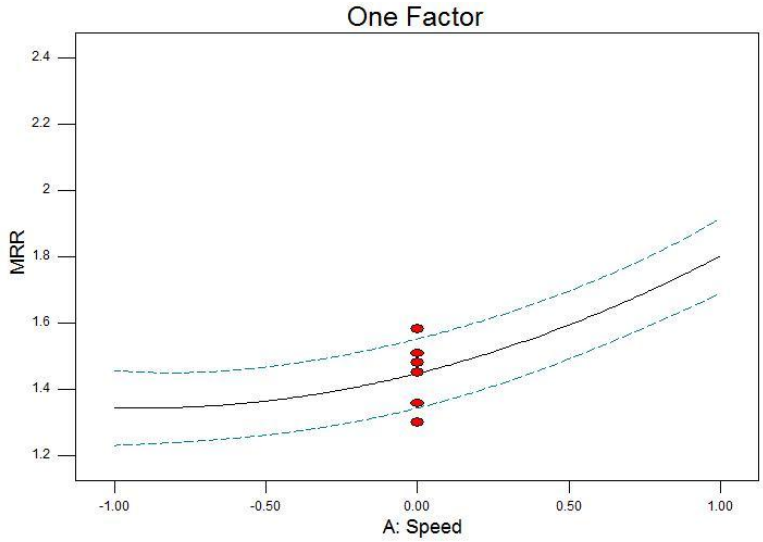

Fig 4.5.15: One Factor-Cutting speed for MRR after Backward Elimination

In one factor-cutting speed (fig 4.5.15) plot, the behavior of one independent variable cutting speed is showing with material removal rate. It implies that as the speed increases material removal rate is flat but as further cutting speed increases the material removal rate increases.

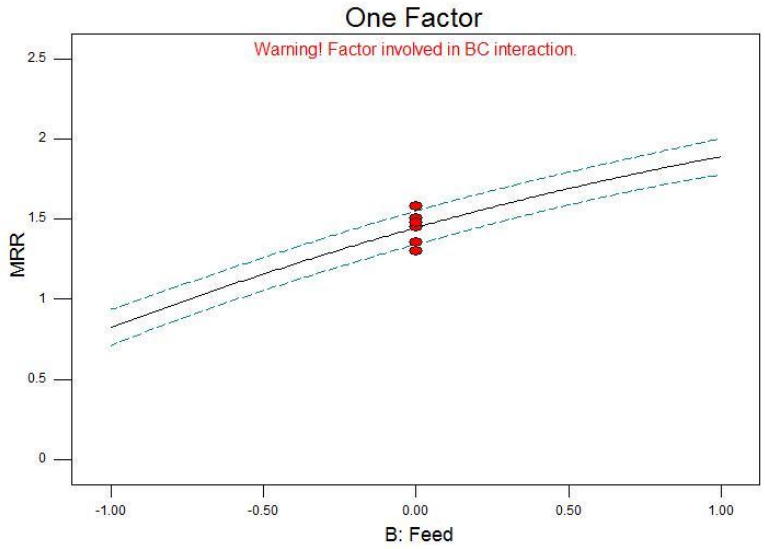

Fig 4.5.16: One Factor-Feed for MRR after Backward Elimination

The behavior of second independent variable feed is showing with respect to material removal rate (fig 4.5.16). It implies that as the feed increases material removal rate increases. The behavior of third independent variable depth of cut is showing with respect to material removal rate (fig 4.5.17). It observed that as the depth of cut increases material removal rate increases.

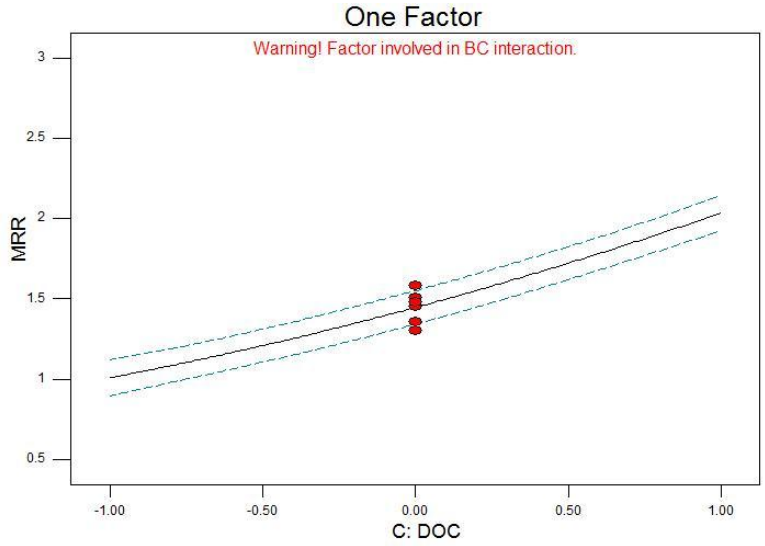

Fig 4.5.17: One Factor-Depth of cut for MRR after Backward Elimination

The graph between cutting speed, feed and depth of cut versus material removal rate at a point have been plotted in perturbation, shown in fig 4.5.18. It implies that as the cutting speed increases, the material removal rate is initially flat and then increases but by increasing the depth of cut and feed, the material removal rate increases.

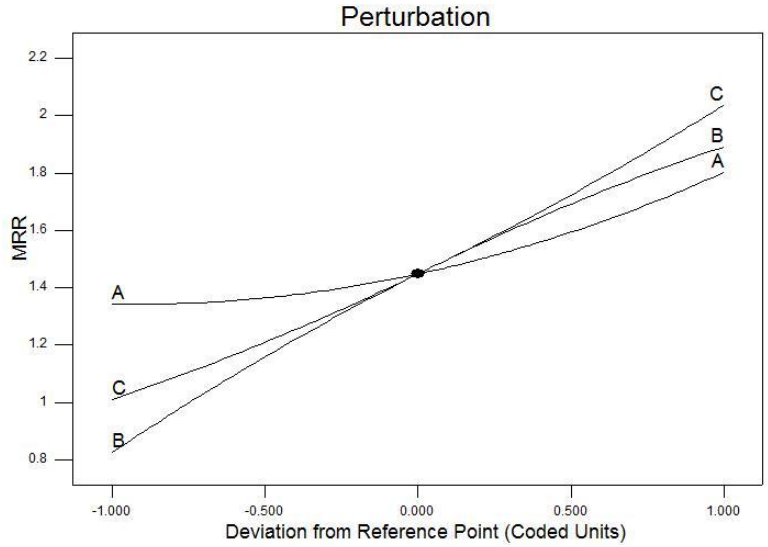

Fig 4.5.18: Perturbation graph for MRR after Backward Elimination

Both contour plot and surface 3D plots help to understand the nature of the relationship between the two factors (Cutting speed, feed and depth of cut) and the response (material removal rate). The contour plots for two different independent variables (feed and depth of cut) and response (material removal rate) is shown in fig 4.5.19.

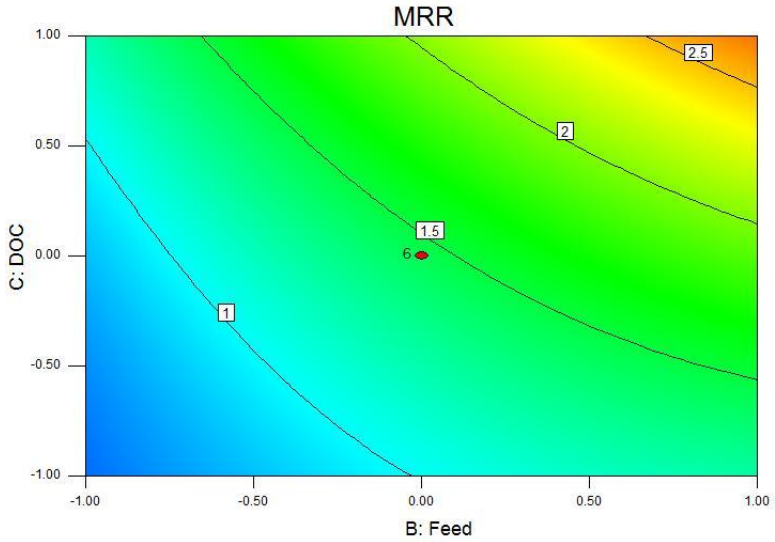

Fig 4.5.19: Response contour plot between Feed and Depth of cut after Backward Elimination

A response surface plot generally displays a three dimensional view that may provide a clearer picture of the response. The response surface 3D plot for two different independent variables (feed and depth of cut) and response (material removal rate) is shown in fig 4.5.20. The behavior of graph indicates that the maximum material removal rate is achieved at about 0.25mm/rev feed and at 1.25mm depth of cut.

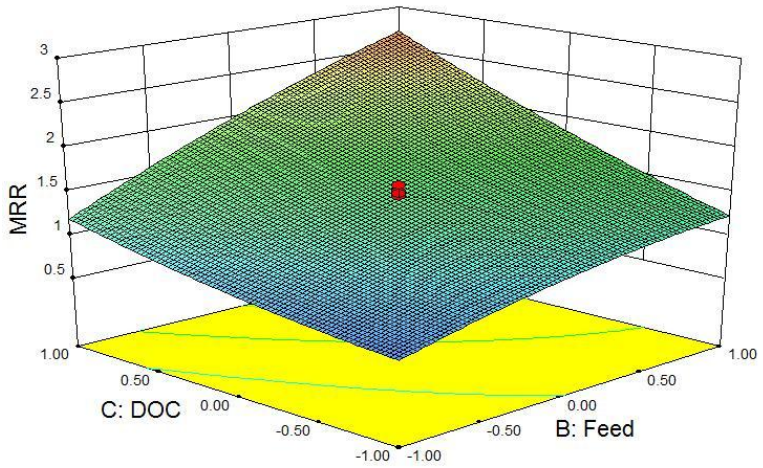

Fig 4.5.20: Response surface plot between Feed and Depth of cut after Backward Elimination

4.5.4 Conclusion

The analysis of the experimental observation highlights that the material removal rate in CNC turning process is greatly influenced by depth of cut followed by feed and cutting speed, with contribution of 42.08%, 39.04% and 7.8% respectively. It is noted that the maximum value of material removal rate is 2.63gm/sec, which is at 2100 rpm cutting speed, 0.15 mm/rev feed and 1.25 mm depth of cut. The minimum value of material removal rate is 0.50 gm/sec, which is at 1800 rpm cutting speed, 0.10 mm/rev feed and 0.50 mm depth of cut. Form the analysis and behavior of surface plots and contour plots, it implies that the optimal condition for higher material removal rate is at 2700 rpm cutting speed, 0.25 mm/rev feed and 1.25 mm depth of cut.

4.6 CASE STUDY 3 FOR TEMP ANALYSIS

The investigated results of chip-tool interface temperature obtained during turning of EN-31 tool steel. The results were obtained at variation of Cutting Speed e.g. from 1800 to 2700 rpm, feed rate e.g. from 0.05 to 0.25 mm/rev, and depth of cut from 0.25 to 1.25 mm. The experiments data are fed into design of experiments and the following table 4.6.1 get.

Table 4.6.1: Design of experiment matrix (coded) for temp

Sl. No.	Std	Run	Factor 1 A: speed (rpm)	Factor 2 B: Feed (mm/rev)	Factor 3 C: DOC (mm)	Response T_{max} (^{O}C)
1	20	1	0.00	0.00	0.00	45
2	13	2	0.00	0.00	-1.68	40
3	7	3	-1.00	1.00	1.00	76
4	2	4	1.00	-1.00	-1.00	41.2
5	6	5	1.00	-1.00	1.00	42.6
6	16	6	0.00	0.00	0.00	46
7	9	7	-1.68	0.00	0.00	37.9
8	17	8	0.00	0.00	0.00	44
9	4	9	1.00	1.00	-1.00	43.5
10	18	10	0.00	0.00	0.00	46.4
11	10	11	1.68	0.00	0.00	42.5
12	14	12	0.00	0.00	1.68	69
13	3	13	-1.00	1.00	-1.00	38.5
14	1	14	-1.00	-1.00	-1.00	37.5
15	8	15	1.00	1.00	1.00	73
16	19	16	0.00	0.00	0.00	45.6
17	5	17	-1.00	-1.00	1.00	39.5
18	12	18	0.00	1.68	0.00	68
19	11	19	0.00	-1.68	0.00	39
20	15	20	0.00	0.00	0.00	47

The coded form of design of experiment matrix is shown in table 4.6.1 and uncoded form of design of experiment matrix is shown in table 4.6.2.

Table 4.6.2: Design of experiment matrix (uncoded) for temp

Sl. No.	Std	Run	Factor 1 A: speed (rpm)	Factor 2 B: Feed (mm/rev)	Factor 3 C: DOC (mm)	Response T_{max} (^{O}C)
1	20	1	2100	0.15	0.75	45
2	13	2	2100	0.15	0.25	40
3	7	3	1800	0.20	1.00	76
4	2	4	2400	0.10	0.50	41.2
5	6	5	2400	0.10	1.00	42.6
6	16	6	2100	0.15	0.75	46

7	9	7	1500	0.15	0.75	37.9
8	17	8	2100	0.15	0.75	44
9	4	9	2400	0.20	0.50	43.5
10	18	10	2100	0.15	0.75	46.4
11	10	11	2700	0.15	0.75	42.5
12	14	12	2100	0.15	1.25	69
13	3	13	1800	0.20	0.50	38.5
14	1	14	1800	0.10	0.50	37.5
15	8	15	2400	0.20	1.00	73
16	19	16	2100	0.15	0.75	45.6
17	5	17	1800	0.10	1.00	39.5
18	12	18	2100	0.25	0.75	68
19	11	19	2100	0.05	0.75	39
20	15	20	2100	0.15	0.75	47

The design summary of chip-tool interface temperature experiments is shown in table 4.6.3. In this table minimum and maximum value of independent variables (cutting speed, feed and depth of cut) and std. dev are shown.

Table 4.6.3: Design summary for temp

Sl. No.	Factor	Name	Units	Type	Subtype	Minimum	Maximum	-1 actual	+1 actual	mean	Std. Dev.
1	A	Speed	rpm	numeric	Continuos	-1.68	1.68	-1.00	1.00	0.00	0.83
2	B	Feed	mm/rev	numeric	Continuos	-1.68	1.68	-1.00	1.00	0.00	0.83
3	C	DOC	mm	numeric	Continuos	-1.68	1.68	-1.00	1.00	0.00	0.83

4.6.1 Result Analysis and Discussion

After design of summary the experimental data are analyzed. During this analysis process get the response range from 37.5 to 76, ratio of max to min 2.02667. Then get the summary of quadratic, shown in table 4.6.4. In this summary get the sequential p-value of quadratic less than 0.0001, lack of fit p-value 0.3273, adjusted R-squared 0.9908 and predicted R-squared 0.9713, and this quadratic is suggested. In this evaluation module, a quadratic fit is done. For response surface quadratic model, no aliases (aliases are calculated based on the response selection, taking into account missing data points) found for quadratic model.

Table 4.6.4: Summary of Quadratic for temp

Sl. No.	Source	Sequential p-value	Lack of fit p-value	Adjusted R-Squared	Predicted R-Squared	
1	Linear	0.0001	0.0001	0.6611	0.4814	
2	2FI	0.0047	0.0006	0.8408	0.7855	
3	**Quadratic**	**<0.0001**	**0.3273**	**0.9908**	**0.9713**	**Suggested**
4	Cubic	0.2991	0.3235	0.9924	0.8954	Aliased

Sequential model sum of square (type-I) get in chip-tool interface temperature analysis process after summary of quadratic table, shown in table 4.6.5. In this table it is clearly mentioned that the design of experiment suggested for quadratic Vs 2FI model. The p-value and F-value for quadratic Vs 2FI are less than 0.0001 and 71.31 respectively.

Table 4.6.5: Sequential Model Sum of Square (Type-1) for temp

Sl. No.	Source	Sum Of Squares	df	Mean Square	F Value	p-value prov>F	
1	Mean Vs Total	46291.44	1	46291.44			
2	Linear Vs Mean	2096.36	3	698.79	13.35	0.0001	
3	2FI Vs Linear	517.75	3	172.58	7.02	0.0047	
4	**Quadratic Vs 2FI**	**305.35**	**3**	**101.78**	**71.31**	**< 0.0001**	**Suggested**
5	Cubic Vs Quad	7.27	4	1.82	1.55	0.2991	Aliased
6	Residual	7.01	6	1.17			
7	Total	49225.18	20	2461.26			

After Sequential model sum of square (type-I) get lack of fit test and model summary statistical in table 4.6.6 and table 4.6.7. In both tables quadratic model is suggested. In lack of fit test the p-value (probability > F) is 0.3273 and F value is 1.52.

Table 4.6.6: Lack of Fit Test for temp

Sl. No.	Source	Sum Of Squares	df	Mean Square	F Value	p-value prov>F	
1	Linear	831.72	11	75.61	66.87	0.0001	
2	2FI	313.98	8	39.25	34.71	0.0006	
3	**Quadratic**	**8.62**	**5**	**1.72**	**1.52**	**0.3273**	**Suggested**
4	Cubic	1.36	1	1.36	1.20	0.3235	Aliased
5	Pure Error	5.65	5	1.13			

The desirable value of R-squared is close to one in model summary statistics, table 4.6.7, which is R^2= 99.51% shows that this much percentage of the variability of result is explained by the model. The predicted R-Squared value of 0.9713 is in reasonable agreement with the adjusted R-squared of 0.9908. PRESS stands for predicted residual error sum of squares and it is a measure of how well the model for the experiment is likely to predict the response in new experiments. In this case PRESS is 84.32. In this table also quadratic is suggested.

Table 4.6.7: Model Summary Statistics for temp

Sl. No.	Source	Std. Dev.	R-Squared	Adjusted R-Squared	Predicted R-Squared	PRESS	
1	Linear	7.23	0.7146	0.6611	0.4814	1521.46	
2	2FI	4.96	0.8911	0.8408	0.7855	629.40	
3	**Quadratic**	**1.19**	**0.9951**	**0.9908**	**0.9713**	**84.32**	**Suggested**
4	Cubic	1.08	0.9976	0.9924	0.8954	306.92	Aliased

After lack of fit test and model summary statistical, get analysis of variance (ANOVA) for response surface quadratic model, shown in table 4.6.8. In this table get the lack of fit and source AB not significant and other sources are getting significant. The model F-value of 227.25 implies the model is significant. There is only a 0.01% chance that a 'model F-value' this large could occur due to noise. On lack of fit, the F value and p-value (probability > F) are 1.52 and 0.3273 (> 0.05). The lack of fit F-value of 1.52 implies the lack of fit is not significant relative to the pure error. Non significant lack of fit is good. This is desirable as it indicates that the terms in the model have significant effect on the response. This implies that the model could fit and it is adequate. Cutting speed, feed, depth of cut and other sources have p-value less than 0.05. After examination of F-values in this table indicate that the variables, cutting speed (A), feed (B) and depth of cut (C), AC, BC, A^2, B^2, C^2 are significant at 95% confidence level. To ensure the validity of lack of fit test, the degree of freedom for lack of fit should be minimum 3 (< 5) and for pure error minimum 4 (< 5).

Table 4.6.8: Analysis of Variance (ANOVA) for temp

Sl. No.	Source	Sum of Squares	df	Mean Square	F Value	p-value prov>F	
1	Model	2919.46	9	324.38	227.25	< 0.0001	
2	A-Speed	20.02	1	20.02	14.03	0.0038	
3	B-Feed	1036.43	1	1036.43	726.09	< 0.0001	
4	C-DOC	1039.91	1	1039.91	728.53	< 0.0001	
5	AB	2.88	1	2.88	2.02	0.1859	
6	AC	9.24	1	9.24	6.48	0.0291	
7	BC	505.62	1	505.62	354.22	< 0.0001	
8	A^2	61.76	1	61.76	43.27	< 0.0001	
9	B^2	99.84	1	99.84	69.94	< 0.0001	
10	C^2	128.46	1	128.46	89.99	< 0.0001	
11	Residual	14.27	10	1.43			
12	**Lack of Fit**	**8.62**	**5**	**1.72**	**1.52**	**0.3273**	**Not significant**
13	Pure Error	5.65	5	1.13			
14	Cor Total	2933.74	19				

Final Equation in terms of coded factors:

The quadratic model for chip-tool interface temperature in terms of coded factors is given below.

T_{max} = + 45.69 + 1.21 *A + 8.71 *B + 8.73 *C – 0.60 *A *B – 1.07 *A *C + 7.95 *B *C – 2.07 *A^2 + 2.63 *B^2 + 2.99 *C^2

Maximum Temperature, T_{max} = +(45.69) + (1.21 * Cutting Speed) + (8.71 * feed) + (8.73 * Depth of Cut) – (0.60 * Cutting Speed * Feed) – (1.07 * Cutting Speed * Depth of Cut) + (7.95 * Feed *Depth of Cut) – (2.07 *Cutting Speed^2) + (2.63 * Feed^2) + (2.99 *Depth of Cut^2)

The normal probability plot of residuals for chip-tool interface temperature is illustrated in Fig 4.6.1. It is expected that data from experiments form a normal distribution. It reveals that the residual fall on a straight line, implying that the errors (residuals) are spread in a normal distribution. This is also, confirmed by the variations between the experimental results and model predicted values analyzed through residual graphs.

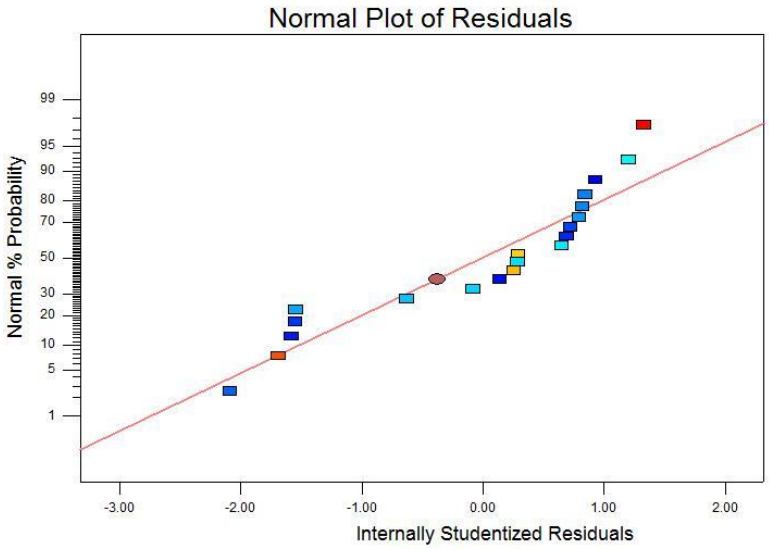

Fig 4.6.1: Normal plot of residual for temperature

The actual and predicted plot shows how well the model fits the data. As seen from the fig 4.6.2, all the data lying on the diagonal line. It implies that this model is fit and gives the desired response.

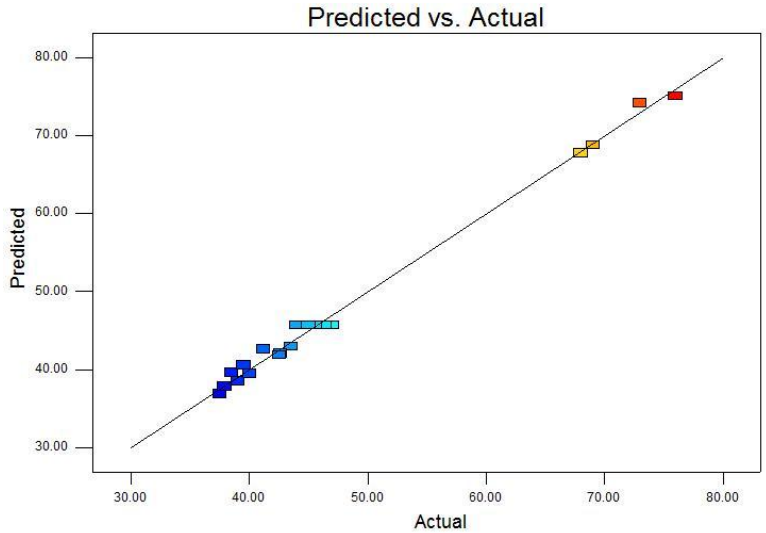

Fig 4.6.2: Predicted Vs actual graph for temperature

To show the effect of independent variables like cutting speed, feed and depth of cut plotted individually graph with respect to response chip-tool interface temperature. These plots are show in fig 4.6.3, fig 4.6.4 and fig 4.6.5.

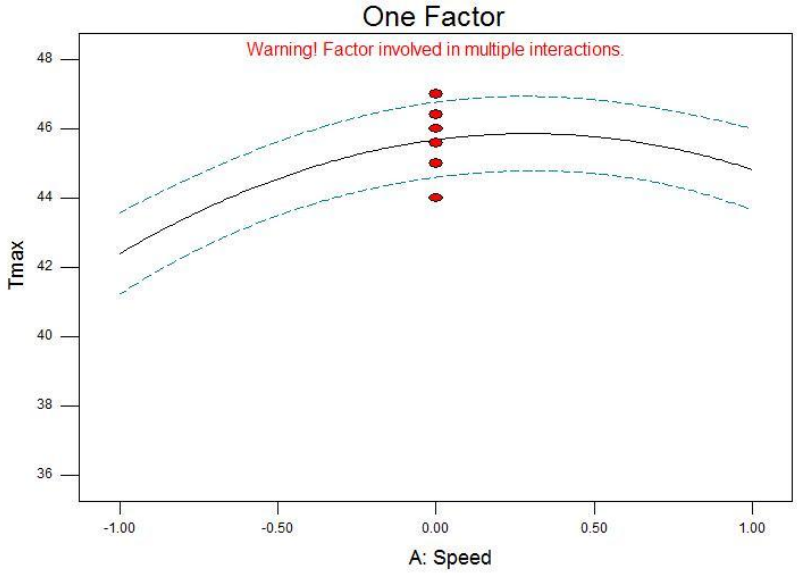

Fig 4.6.3: One factor- cutting speed plot for temperature

In one factor-cutting speed (fig 4.6.3) plot, the behavior of one independent variable cutting speed is showing with response chip-tool interface temperature. It implies that as the cutting speed increases chip-tool interface temperature increases bur further as the cutting speed increases chip-tool interface temperature decreases.

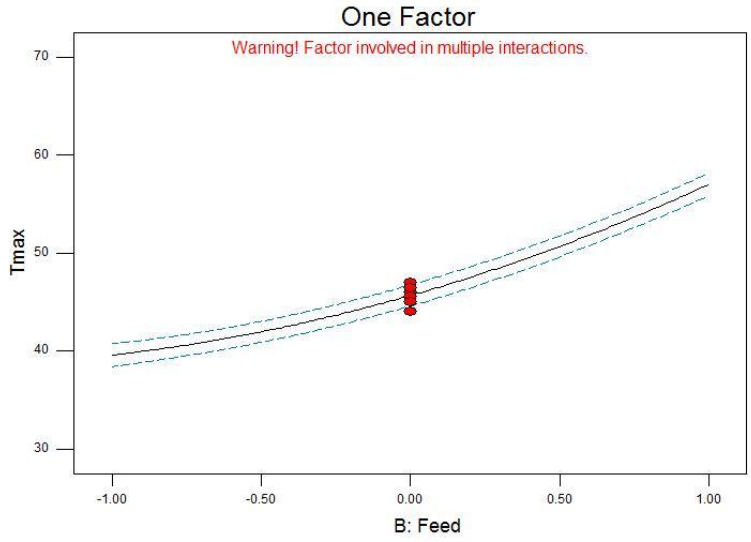

Fig 4.6.4: One factor- feed plot for temperature

In other one factor-feed (fig 4.6.4) plot, the behavior of one independent variable feed is showing with response chip-tool interface temperature. It implies that as the feed increases chip-tool interface temperature increases.

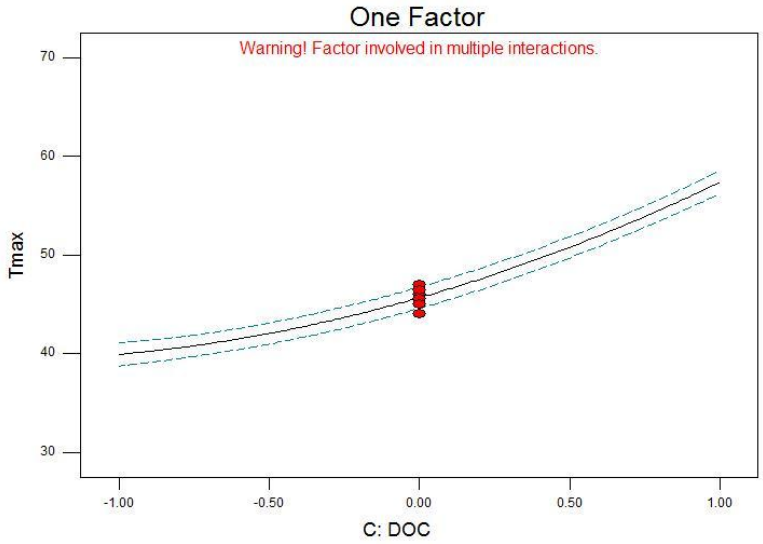

Fig 4.6.5: One factor- depth of cut plot for temperature

In third one factor-depth of cut (fig 4.6.5) plot, the behavior of one independent variable feed is showing with response chip-tool interface temperature. It implies that as the depth of cut increases chip-tool interface temperature increases.

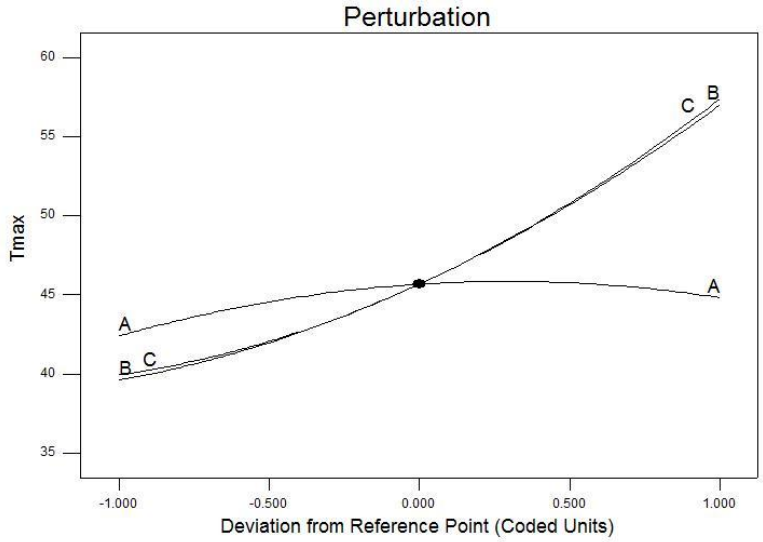

Fig 4.6.6: Perturbation plot for temperature

The graph between cutting speed, feed and depth of cut versus chip-tool interface temperature have been plotted at one point in perturbation, shown in fig 4.6.6. In this plot, the behavior of independent variable with respect to chip-tool interface temperature at a point is shown. It implies that as the cutting speed increases, the chip-tool interface temperature initially increases and then decreases but by increasing the depth of cut and feed, the chip-tool interface temperature increases.

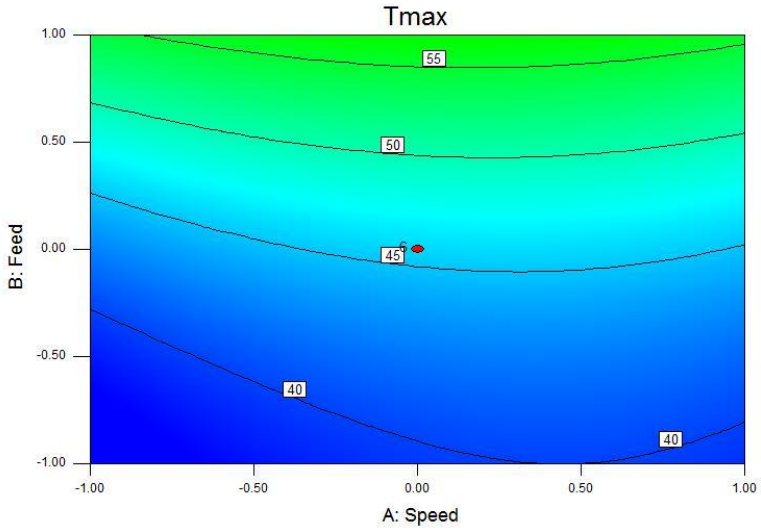

Fig 4.6.7: Response contour plot between cutting speed and feed for temp.

To convert the experimental data into informative map with quantitative information about the model uses response contour plot. Contour plot is generated for two factors (independent variables). The typical application of the contour plot is in determining settings that will maximize (or minimize) the response variable. The contour plots for two different independent variables and response (chip-tool interface temperature) are shown in fig 4.6.7, fig 4.6.8 and fig 4.6.9. The contour plots for two different independent variables (cutting speed and feed) and response (chip-tool interface temperature) are shown in fig 4.6.7.

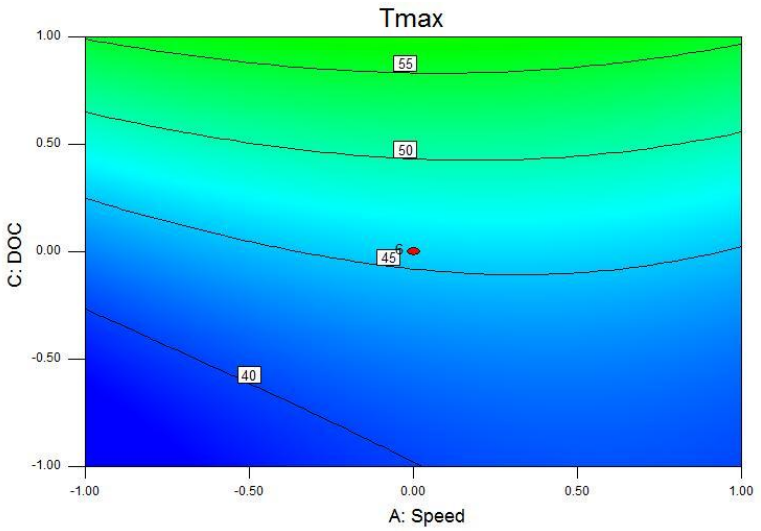

Fig 4.6.8: Response contour plot between cutting speed and depth of cut for temp.

The contour plots for two different independent variables (cutting speed and depth of cut) and response (chip-tool interface temperature) are shown in fig 4.6.8. The contour plots for two different independent variables (feed and depth of cut) and response (chip-tool interface temperature) are shown in fig 4.6.9

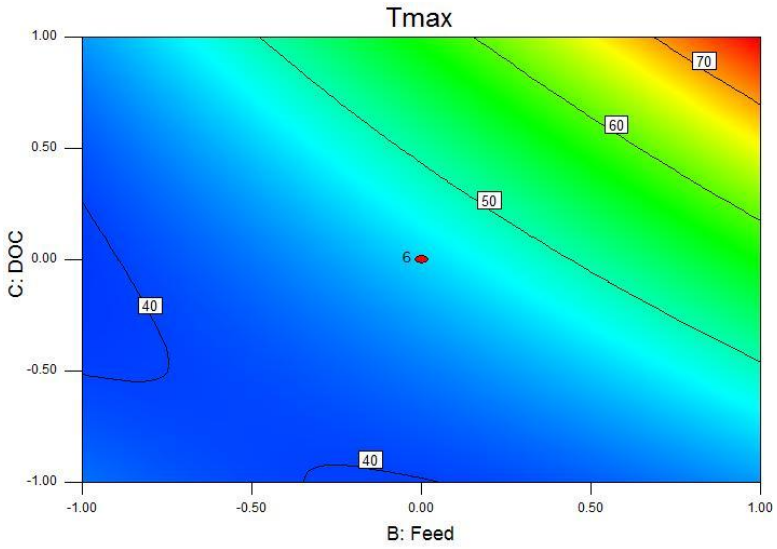

Fig 4.6.9: Response contour plot between feed and depth of cut for temp.

A response surface plot generally displays a three dimensional view that may provide a clearer picture of the response. If the regression model (first order model) contains only the main effect and no interaction, the fitted response surface will be a plane (contour lines will be straight). If the model contains interaction effect, the contour lines will be curved and not straight. The response surface 3D plot for two different independent variables and response chip-tool interface temperature are shown in fig 4.4.10, fig 4.4.11 and fig 4.4.12.

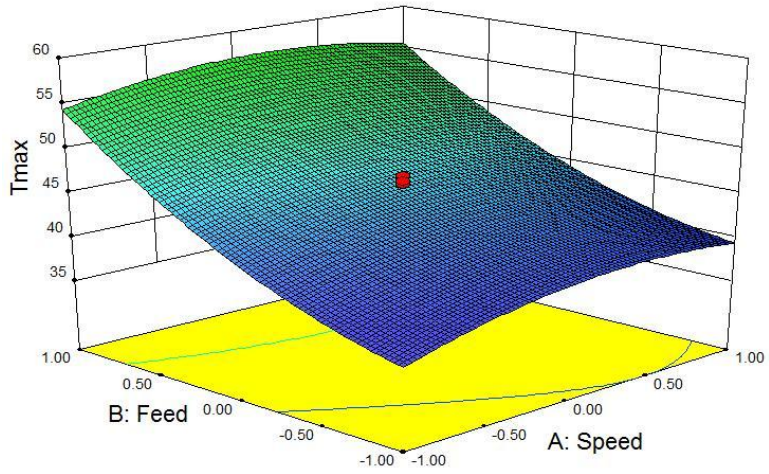

Fig 4.6.10: response surface plot between cutting speed and feed for temp

The response surface 3D plot for two different independent variables (cutting speed and feed) and response chip-tool interface temperature is shown in fig 4.4.10. It indicates that as cutting speed increase chip-tool interface temperature increases but further it decreases, and as the feed increases chip-tool interface temperature increases.

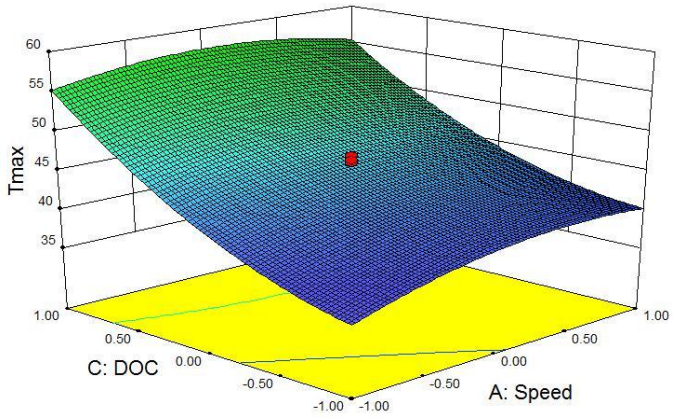

Fig 4.6.11: Response surface plot between cutting speed and depth of cut for temp

The response surface 3D plot for two different independent variables (cutting speed and depth of cut) and response chip-tool interface temperature is shown in fig 4.4.11. It indicates that as cutting speed increase chip-tool interface temperature increases but further it decreases, and as the depth of cut increases chip-tool interface temperature increases.

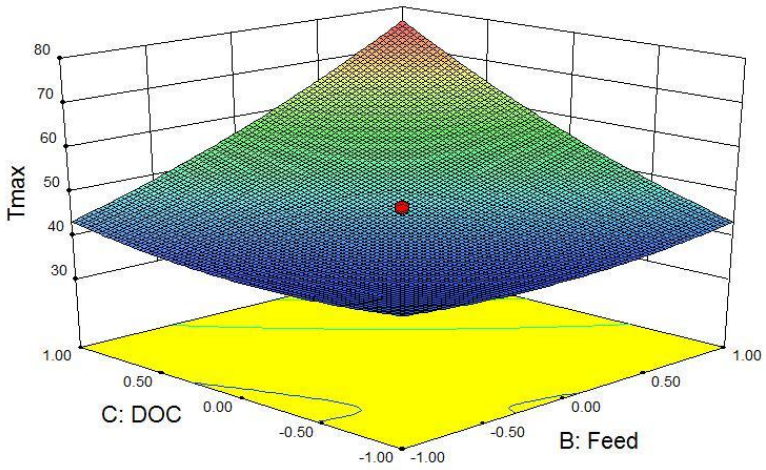

Fig 4.6.12: Response surface plot between feed and depth of cut for temp

The response surface 3D plot for two different independent variables (feed and depth of cut) and response chip-tool interface temperature is shown in fig 4.4.12. It indicates that as feed increase chip-tool interface temperature increases and as the depth of cut increases chip-tool interface temperature increases.

4.6.2 Conclusion

In this case study the chip-tool interface temperatures have been experimentally studied with infrared camera in CNC turning process. The model developed in this case study produces small errors and has satisfactory result. This model has the regression coefficient

approximate 0.99 (R-squared=99.51%). Therefore the proposed model can be utilized to predict the corresponding chip-tool interface temperatures of EN-31 tool steel at different parameters in turning. This can also be used for metal cutting process optimization, increasing productivity and reducing manufacturing cost. The analysis of the experimental observation highlights that the chip-tool interface temperature is influenced by depth of cut and feed, with contribution of 35.45% and 35.32% respectively. It is noted that the maximum value of chip-tool interface temperature is 76^0C, which is at 1800rpm cutting speed, 0.20 mm/rev feed and 1.00 mm depth of cut. The minimum value of chip-tool interface temperature is 37.5^0C, which is at 1800rpm cutting speed, 0.10 mm/rev feed. and 0.50 mm depth of cut. From the analysis and behavior of contour plot and surface plot, it implies that the optimal condition for higher chip-tool interface temperature is at 2100rpm cutting speed, 0.25 mm/rev feed and 1.25 mm depth of cut.

CHAPTER 5

CONCLUSION

In this project surface roughness, material removal rate and chip-tool interface temperature have been experimentally studied on CNC machine with coated carbide insert. The process design of twenty experiments has been carried out with the help of design of experiments in response surface methodology. The successful optimization of all responses (surface roughness, material removal rate and chip-tool interface temperature) has been achieved. From the above three case study, the following has been conclude.

1. For surface roughness the feed is dominating factor. By increasing feed and depth of cut surface roughness increases. But as the cutting speed increases surface roughness decreases.
2. The contribution of feed 50.49%, depth of cut 17.16% and cutting speed 23.04% get in the surface roughness case study.
3. The optimum value of turning parameters is 2700 rpm cutting speed, 0.05 mm/rev feed and 0.25 mm depth of cut for minimum surface roughness.
4. In the material removal rate case study depth of cut is a major parameter. It is found the as the depth of cut and feed increases the material removal rate increases, but by increasing cutting speed the material removal rate initially flat and then increases.
5. The contribution of depth of cut, feed and cutting speed is 42.08%, 39.04% and 7.8% respectively in case of material removal rate.
6. The optimum value of turning parameters for higher material removal rate is 2700 rpm cutting speed, 0.25 mm/rev feed and 1.25 mm depth of cut.
7. In case of chip-tool interface temperature depth of cut and feed play a major role. It is observed that the chip-tool interface temperature increases by increasing depth of cut and feed, but in case of cutting speed initially chip-tool interface temperature increasing up to a point and then decreasing.
8. In chip-tool interface temperature case study, it is observed that depth of cut and feed contributed 35.45% and 35.32% respectively.
9. The optimum value of turning parameters is 2100rpm cutting speed, 0.25 mm/rev feed and 1.25 mm depth of cut in case of chip-tool interface temperature.

REFERENCES

1. L. B. Abhang and M. Hameedullah, "Power Prediction Model for Turning EN-31 Steel Using Response Surface Methodology", Journal of Engineering Science and Technology Review, Volume 3, issue 1, pp 116-122 (2010).

2. Ashish Yadav, Ajay Bangar, Rajan Sharma, Deepak Pal, "Optimization of Turning Process Parameters for Their Effect on EN-8 Material Work-Piece hardness by using Parameteric Optimization Method", International Journal of Mechanical and Industrial Engineering (IJMIE), Volume 1, Issue-3, pp 36-40 (2012).

3. Ishwer Shivakoti, Sunny Diyaley, Golam Kibria, B.B. Pradhan, " Analysis of Material Removal Rate using Genetic Algorithm Approach", International Journal of Scientific & Engineering Research, volume 3, issue 5, pp 747-752 (2012).

4. C. X. Feng and X. Wang, "Development of Empirical Models for Surface Roughness Prediction in Finish Turning", International Journal of Advanced Manufacturing Technology, Volume 20, Issue 5, pp 348–356 (2002).

5. K. Adarsh Kumar, Ch.Ratnam, BSN Murthy, B.Satish Ben, K. Raghu Ram Mohan Reddy, "Optimization Of Surface Roughness in Face Turning Operation in Machining of EN-8", international journal of engineering science & advanced technology (IJESAT), Volume 2, Issue 4, pp 807–812 (2012).

6. Panda, A. Dutta, S.K Sahoo, A.K Rout, A.K Routra, B.C, "Experimental investigation on surface roughness characteristics in hard turning of EN31 steel using coated carbide insert: Taguchi and mathematical modeling approach", 5th International & 26th All India Manufacturing Technology, Design and Research Conference (AIMTDR 2014), IIT Guwahati, Assam, December 12th–14th, (2014).

7. H. K. Dave, L. S. Patel and H. K. Raval, "Effect of machining conditions on MRR and surface roughness during CNC Turning of different Materials Using TiN Coated Cutting Tools – A Taguchi approach", International Journal of Industrial Engineering

Computations, Volume 3, Issue 5, pp 925-930 (2012).

8. U.K. Vates and N.K. Singh, "Optimization of Surface Roughness Process Parameters of Electrical Discharge Machining of EN-31 by Response Surface Methodology", International Journal of Engineering Research and Technology, Volume 6, pp. 835-840 (2013).

9. Singaram Lakshmanan, Mahesh Kumar, Al Mussanah College of Technology, Oman, "Optimization of EDM parameters using Response Surface Methodology for EN31 Tool Steel Machining", International Journal of Engineering Science and Innovative Technology (IJESIT), Volume 2, Issue 5, pp 64-71(2013).

10. L B Abhang and M Hameedullah, "Modeling and Analysis for Surface roughness in Machining EN-31 steel using Response Surface Methodology", International Journal of Applied Research in Mechanical Engineering, Volume 1, Issue 1, pp 33-38 (2011).

11. J. Paulo Davim, "Machining of hard materials", Springer London Dordrecht Heidelberg, NY.

12. Prasanna P Kulkarni, Shreelakshmi C. T., Shruti V. Harihar, Radha Bai, "An Experimental Investigation of effect of cutting fluids on chip formation and cycle time in turning of EN-24 and EN-31 material", International Journal of Engineering Research and Technology, ISSN: 2277-9655, Volume 3, issue 11, pp 566-573 (2014).

13. Boothroyd, G. and Knight, W.A., "Fundamentals of machining and machine tools", second Edition, Marcel Dekker Inc., New York (1989).

14. Harish Kumar, Mohd. Abbas, Dr. Aas Mohammad, Hasan Zakir Jafri, " Optimization of cutting parameters in CNC turning", International Journal of engineering research and application, ISSN: 2248-9622, Volume 3, Issue 3, pp. 331-334 (2013).

15. Richard Geo and Jose Sheril D'cotha, " Effect of turning parameters on power consumption in EN-24 alloy steel using different tools", International journal of engineering research and general science, Volume 2, Issue 6, pp. 691-702 (2014)

16. C.R.Barik and N.K.Mandal, "Parametric Effect and Optimization of Surface Roughness of EN-31 in CNC Dry Turning", International Journal of Lean Thinking, Volume 3, Issue 2, pp. 54-66 (2012).

17. Nirpaksh Uppal, Rohit Rampal and Charanjeet Singh Sandhu, " To Analyses The Effects of Turning Parameters on Material Removal Rate of AISI 4041 Die Alloy Steel", International Journal of Research in Engineering and Technology, Volume 2, Issue 9, pp. 538-541 (2013).

18. S. Thamizhmanii, S. Saparudin, S. Hasan, " Analyses of Surface roughness by turning process using Taguchi method", Journal of Achievements in Material and Manufacturing Engineering, Volume 20, Issues 1-2, pp 503-506 (2007).

19. S.S.Acharya, R.L.Karwande, " Review on Investigation and optimization of turning process parameter in wet and MQL system on EN-31", International Journal of research in Engineering and Technology, Volume 3, Issue 7, pp 50-52 (2014).

20. L.B.Abhang and M.Hameedullah, " Chip-tool interface temperature prediction model for turning process", International Journal of Engineering science and Technology, Volume 2, Issue 4, pp 382-393 (2010).

21. http://www.statease.com/pubs/doesimp2excerpt--chap3.pdf (pp. 3–21 to 3–25).

22. http://textofvideo.nptel.iitm.ac.in/112105126/lec5.pdf (pp 2-5).

23. K. Krishnamurthy and J.Venkatesh, “Assessment of surface roughness and material removal rate on machining of TIB2 reinforced aluminum 6063 composites : A Taguchi’s approach”, International Journal of scientific and Research Publications, Volume 3, Issue 1, pp 1-6 (2013).

24. Awadhesh Pal, S.K. Choudhury, Satish Chinchanikar, “Machinability assessment through experimental investigation during hard and soft turning of hardened steel”, 3rd International Conference on Materials Processing and Characterisation (ICMPC 2014), Volume 6, pp 80-91 (2014).

25. S. Harish, A.Bensely, D. Mohan Lal, A.Rajadurai, G. B. Lenkey, “Microstructural study of cryogenic treated EN-31 bearing steel”, Journal of Materials Processing Technology, Volume 209, Issue 7, pp 3351-3357 (2009).

26. S. R. Das, R. P. Nayak, D. Dhupal, “Optimization of cutting parameters on tool wear and eork-piece surface temperature in turning of AISI D2 steel”, International Journal of Lean Thinking, Volume 3, Issue 2, pp 140-156 (2012).

27. Adeel H. Suhail, N. Ismail, S. V. Wong and N. A. Abdul Jalil, “Optimization of cutting parameters based on surface roughness and assistance of work-piece surface temperature in turning process”, American Journal of Engineering and Applied Sciences, Volume 3, Issue 1, pp 102-108 (2010).

28. N. H. Rafai & M. N. Islam, “An Investigation Into Dimensional Accuracy And Surface Finish Achievable In Dry Turning”, Machining Science and Technology, Volume 13, Issue 4, pp 571 - 589 (2009).

29. C. Ming, Sun Fanghong, W. Haili and Y. Renwei, “Experimental research on the dynamic characteristics of the cutting temperature in the process of high-speed milling”, Journal Materials Processing technology, Volume 138, Issue 1-3, pp 468-471 (2003).

30. K.S.Park and S. H. Kim, “Artificial intelligence approaches to determination of-CNC machining parameters in manufacturing: A Review”, Artificial Intelligence in Engineering, Volume 12, Issue 1, pp 121-134 (1998).

31. Ashok kumar Sahoo and Bidyadhar sahoo, “Surface roughness model and parametric optimization in finish turning using coated carbide insert: Response surface methodology and Taguchi approach”, International Journal of Industrial Engineering Computations, Volume 2, Issue 4, pp 819-830 (2011).

32. A. Belloufi, M. Assas, I. Rezgui, “Optimization of turning operations by using a hybrid genetic algorithm with sequential quadratic programming”, Journal of Applied Research and Technology, Volume 11, pp 88-94 (2013).

33. M. C. Chen and K. V. Chen, “Optimization of multipass turning operations with genetic algorithm: A Note”, International Journal of Production Research, Volume 41, Issue 14, pp 3385-3383 (2003).

34. Aslan, E., Camuscu, N. and Birgoren, B., “Design optimization of cutting parameters when turning hardened AISI 4140 steel (63 HRC) with Al2O3 + TiCN mixed ceramic tool”, Materials & Design, Volume 28, Issue 5, pp 1618-1622 (2007).

35. Dilbag singh, P. V. Rao, “A surface roughness prediction model for hard turning process”, International Journal Advanced Manufacturing Technology, Volume 32, pp 1115-1124 (2007).

36. Ashish Bhateja, “Optimization of different performance parameters i.e. surface roughness, tool wear rate & material removal rate with the selection of various process parameters such as speed rate, feed rate, specimen wear, depth of cut in CNC turning of EN 24 alloy steel – An empirical approach”, International Journal of Engineering and Science, Volume 2, Issue 1, pp 103-113 (2013).

37. Chetan Darshan, Lakhvir Singh & APS sethi, “Analysis and optimization of

ceramic cutting tool in hard turning of EN-31 using factorial design", International Journal of Mechanical and Industrial Engineering, Volume 1, Issue 4, pp 49-54 (2012).

38. W. Grzesik, T. Wanat, "Surface finish generated in hard turning of quenched alloy steel parts using conventional and wiper ceramic inserts", International Journal of Machine Tools and Manufacture, Volume 46, Issue 15, pp 1988-1995 (2006).

39. Meena gupta & Surinder Kumar, "Investigation of surface roughness and MRR for turning of UDGFRP using PCA and Taguchi method", International Journal of Engineering Science and Technology, Volume 18, pp 70-81 (20015).

40. S. Gopalakannan, T. Senthilvelan, "Optimization of machining parameters for EDM operations based on central composite design and desirability approach", International Journal of Engineering Science and Technology, Volume 28, Issue 3, pp 1045-1053 (2014).

41. S. A. Hussain, V. Pandurangadu, K. Palanikumar, "Machinability of galss fiber reinforced plastic (GFRP) composite materials", International Journal of Engineering Science and Technology, Volume 3, Issue 4, pp 103-118 (2011).

42. M. Thiyagu, L. Karunamoorthy, N. Arunkumar, "Experimental studies in machining duplex stainless using Response Surface Methodolgy", International Journal of Mechanical & Mechatronics Engineering, Volume 14, Issue 3, pp 48-61 (2014).